LAMINAR FLAME SPEED MEASUREMENTS OF SYNTHETIC GAS BLENDS WITH HYDROCARBON IMPURITIES

A Thesis

by

CHARLES LEWIS KEESEE

Submitted to the Office of Graduate and Professional Studies of
Texas A&M University
in partial fulfillment of the requirements for the degree of

MASTER OF SCIENCE

Chair of Committee,	Eric L. Petersen
Committee Members,	M. Sam Mannan
	Gerald Morrison
Head of Department,	Andreas A. Polycarpou

May 2015

Major Subject: Mechanical Engineering

ABSTRACT

New laminar flame speed measurements have been taken for a wide range of synthetic gas, or syngas, mixtures. These experiments began with two baseline mixtures. The first of these baseline mixtures was a bio-syngas surrogate with a 50/50 H_2/CO split, and the second baseline mixture was a coal syngas blend with a 40/60 H_2/CO split. Experiments were conducted over a range of equivalence ratios from φ = 0.5 to 3 at initial conditions of 1 atm and 296 K. Upon completion of the baseline experiments, two different hydrocarbons were added to the fuel mixtures at levels ranging from 0.8 to 15% by volume, keeping the H_2/CO ratio locked for the bio-syngas and coal syngas mixtures. The addition of these light hydrocarbons, namely CH_4 and C_2H_6, had been shown in a previous numerical study to have significant impacts on the laminar flame speed, and the present experiments validated the suspected trends. For example, a 7% addition of methane to the coal-syngas blend decreased the peak flame speed by about 25% and shifted it from φ = 2.2 to a leaner value near φ = 1.5. Also, the addition of ethane at 1.7% reduced the mixture flame speed more than a similar addition of methane (1.6%). Images taken during the experiments show the addition of hydrocarbons increasing the stability of the flame. The analysis also looked at the effects of hydrocarbon addition on the Markstein lengths and Lewis numbers of the mixtures. Markstein lengths were relatively consistent throughout all mixtures investigated. The Lewis numbers were found to move closer to unity for both lean and rich mixtures as hydrocarbons were added. Compared to the experimental results the model predicts the shape of the flame

speed curve and places the peak at the correct equivalence ratio. However the model predicts a slower flame speed when hydrocarbons are added.

ACKNOWLEDGMENTS

I would like to thank my advisor Dr. Eric Petersen. He has always been there to answer questions or provide direction as needed throughout this project. He took me in as a graduate student as I left the Army, and I have not looked back or regretted the decision. Also thanks to Dr. Mannan and Dr. Morrison for serving on my committee.

I also would like to thank all of my colleagues at the lab, especially the flame speed group; Anabal, Sankar, and Travis. The countless hours we spent discussing anything from the major concepts of flame speed to the minor details of the experimental set up helped immensely.

I also must thank Dr. Kuiwen Zhang and our partners at the National University of Ireland at Galway. Their work on the flame sensitivity analysis contributed greatly to the project on which this thesis is based.

I also must thank CAPT Mike Sexton, one of my former advisors at VMI, who encouraged me to go to graduate school when I was preparing to leave the Army and specifically recommended I look at Texas A&M.

I want to thank the U.S. Department of Energy for providing the direct funding for this research through the UTSR program. Finally, thanks to the Department of Veterans Affairs for picking up a big portion of my funding through the GI Bill.

NOMENCLATURE

φ	Equivalence Ratio
φ_{Ω}	Oxygen Equivalence Ratio
$\overline{\varphi}$	Normalized Equivalence Ratio
Ω	Oxygen Ratio
S_b	Burned Gas Flame Speed
S_b^0	Unstretched Burned Flame Speed
$S_{L,u}^0$	Laminar unburned, unstretched Flame Speed
σ	Density Ratio
L_b	Burned Markstein Length
r_f	Flame Radius
Le	Lewis Number
Le_v	Volume based, effective Lewis Number
Le_i	Species Lewis Number
X_i	Species Mole Fraction
N_f	Number of Moles, Fuel
N_O	Number of Moles, Oxygen
$N_{O,ST}$	Number of Moles, Oxygen, Stoichiometric

N_{ox}	Number of Moles, Oxidizer
U_{SL}	Total Uncertainty
B_{SL}	Bias Error
P_{SL}	Random Error
$\overline{X}$	Average Difference
SD_{dif}	Standard Dieviation of Difference

TABLE OF CONTENTS

Page

LIST OF FIGURES

Page

LIST OF TABLES

Page

1. INTRODUCTION

Synthetic gas, or syngas, is a mixture primarily composed of CO and H_2. This high-hydrogen combination causes it to be an attractive fuel for power generation through gas turbines. However, the concentrations of each species will vary depending on the feedstock and the process used to gasify it. Ideally, the syngas mixture would just consist of CO and H_2, but rarely is the mixture this simple. As the composition of syngas can vary greatly, it is important to look at all possible and likely impurities individually to fully understand their effects. This approach will allow gas turbine manufacturers the freedom to design safe and efficient turbines that can operate with a variety of syngas mixtures.

Previous studies have shown that there are several impurities that can be present in typical syngas blends. The study of Mathieu et al. [1] focused on the effects of nitrogen- and sulfur-based impurities. A detailed review of several previous studies of syngas mixtures can be found in Lee et al. [2]. However, the individual effects of small hydrocarbons, commonly found in syngas mixtures have not been well studied experimentally with respect to fundamental combustion parameters such as laminar flame speed and ignition delay time. The recent modeling study by Mathieu et al. [1] built upon their results presented in [3], where the previous work had looked specifically at the effects of hydrocarbon addition to syngas for fuel-air mixtures at engine conditions from a numerical perspective. They found that realistic levels of smaller hydrocarbons present in the syngas fuel blend, up to about 15% by volume, can significantly decrease

the laminar flame speed by as much as a factor of two in some cases. The current study builds on the flame speed and ignition delay time modeling research of Mathieu et al. [3] to gain an experimental understanding of the effects of hydrocarbon impurities on the flame speed of syngas mixtures and to help validate the chemical kinetics mechanism. The present study therefore focuses on the hydrocarbons shown in [3] to be present in the largest concentrations and to have the greatest impact on the flame speed, namely methane and ethane.

This thesis begins with a background on the experimental techniques used for outwardly propagating spherical flames followed by an overview of previous work with syngas mixtures. This leads into a brief overview of the mixtures investigated in Section 3. The experimental setup and procedures used are covered in Section 4. The new experimental results for syngas-based laminar flames speeds with and without hydrocarbon impurities along with the results of a modern chemical kinetics model are covered in Section 5. Section 6 provides a detailed analysis of the results. This section begins with a comparison of the experimental results to the model predictions. This topic is followed by a discussion on the thermal-diffusive nature of the flames as well as an analysis of the chemical kinetics. This section also looks at the visible effects of the hydrocarbon addition with an image analysis. The section concludes with a discussion of the Markstein lengths and Lewis numbers of the mixtures investigated. The concluding remarks and plans for future experiments are covered in Section 7.

2. BACKGROUND

As shown below, there are many different methods for experimentally measuring flame speed. The experiments in this study were conducted using an outwardly propagating spherical flame, in a constant volume bomb. As noted by Lowry [4], the advantage of this method over others such as, Bunsen burners and flat flames, is there are no flowing gases. This approach utilizes premixed gases and hence eliminates the uncertainties in equivalence ratio that could be due to imprecise mass flow rates.

Syngas research has been ongoing for a long time. As pointed out by Wender [5], syngas chemistry goes back to the early 20^{th} century. However, because of the wide range of sources for production, and since syngas is a clean fuel, it continues to be an attractive fuel for researchers, as shown by the methods used and the conditions looked at very considerably. As stated in the introduction the work by Lee et al [2], opens with a table containing syngas experiments from 24 separate published works. This compilation includes experiments using various types of equipment, including Bunsen burners, rapid compression machines, and constant-volume bombs. These experiments cover a wide range of temperatures, pressures, and equivalence ratios. These experiments are mostly different CO/H_2 blends with possible dilution of CO_2, He, N_2, Ar, or H_2O. This list is in no way all-inclusive as it focused on recent experiments. Below is a brief summary of some of the experiments that have been conducted, with the attempt to highlight some of the various methods employed and to show where some of the research is going and some of the holes that still need investigated.

The effects of positive flame stretch on outwardly propagating spherical flames was investigated by Hassan et al. [6]. This study looked at a wide range of equivalence ratios going from 0.6 to 5.0 and pressures, from 0.5 atm to 4 atm. These mixtures only consisted of H_2 and CO with the percentage of H_2 ranging from 3-50% by volume.

High-pressure, lean CO/H_2 mixtures were investigated by Goswami et al. [7], using the heat flux method. This method is attractive because it creates a flame very close to the one-dimensional, adiabatic, unstretched state. These experiments filled a void in data for lean, high-hydrogen-content, high-pressure syngas flames.

The study of Bouvet et al. [8] looked at multiple syngas mixtures, changing the ratio of CO/H_2. The four ratios included in this study were: 50/50, 25/75, 10/90, and 5/95. This study also looked at equivalence ratios ranging from the very lean, 0.4, to the very rich, 5.0. These experiments were conducted on an outwardly propagating, spherical flame.

Moist syngas/air mixtures were investigated by Das et al. [9]. For these experiments, steam was added to the syngas mixture of various ratios of H_2/CO, accounting for up to 35% of the fuel mixture.

Syngas mixtures of CO and H_2 heavily diluted with N_2 and CO_2 were investigated by Burbano et al. [10]. The flames in this study were generated using contoured slot-type nozzle burners.

The work described in Gersen et al. [11], focused on auto-ignition of syngas and syngas CH_4 mixtures. These experiments were conducted in a rapid compression machine at engine conditions of high pressure and temperature, with equivalence ratios

of 0.5 and 1.0. The only blend including CH_4 along with both CO/H_2 had a ratio of 0.5/0.3/0.2, respectively.

The research of Monteiro et al. [12] looked at three multicomponent fuels consisting of H_2, CO, CH_4, CO_2, and N_2. These experiments were conducted in a constant-volume, rectangular chamber.

The study of Natarajan, et al [13] discussed the presence of hydrocarbons and other impurities in syngas mixtures and commented on the impact they could have on combustor performance. The study then focused on the effect of CO_2 dilution on a wide range of H_2:CO ratio fuels at high temperatures and pressures. Two separate experimental methods were used to measure flame speed, a Bunsen burner and a wall stagnation flame.

The work of Xu et al.[14] focused on the way syngas is produced and the impurities caused by the production methods and the feedstock used. This study acknowledged that most research was done with a "clean" syngas consisting of only CO, CO_2, and H_2. They found that many other impurities such as: CH_4, C_2H_2, C_2H_6, $C_{10}H_8$, NH_3, HCN, H_2S, COS, SO_2, and NO_X were typically present. It also pointed out that at the time of its printing, 55% of the syngas produced came from coal, and syngas produced from biomass was also found to contain several impurities.

As can be seen, all of the research in syngas aims to fill another void in the current data. While multiple groups have stated impurities are present, this topic has not been experimentally investigated with any rigor. The experimental data presented below is an initial step to fill this lack of experimental data for syngas mixtures with impurities.

3. MIXTURES INVESTIGATED

As mentioned above, the mixtures chosen in this study were based off of two previous numerical studies done in the author's laboratory as presented in Mathieu et al. [1, 3]. These prior studies included two baseline syngas mixtures. These two blends were chosen to represent a nominal coal syngas and a nominal bio-syngas fuels. All ratios and percentages presented in this study are on a molar basis. The coal syngas has a 60/40 ratio of CO to H_2, while the bio-syngas has a 50/50 ratio. Hydrocarbons were then added to each mixture while holding the ratio of CO to H_2 constant. The previous numerical study looked at the addition of four hydrocarbons, CH_4, C_2H_2, C_2H_4, and C_2H_6, with methane being added at various percentages. The study also looked at the combined effect with all four added together at their respective percentages. The predicted flame speeds are shown in Figure 1 and Figure 2.

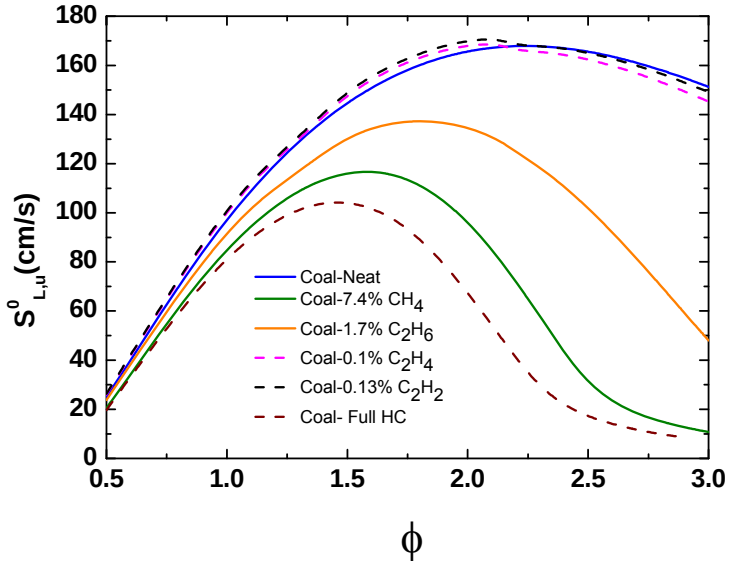

Figure 1. Model predictions for laminar flame speed for coal-syngas blends with hydrocarbon addition at 1 atm and 298 K. [3]. Solid lines indicate mixtures investigated in this study.

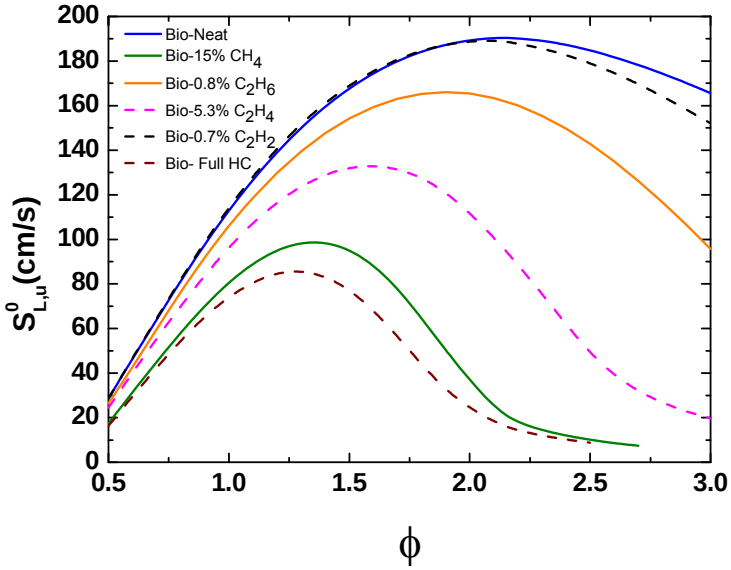

Figure 2. Model predictions for laminar flame speed bio-syngas blends with hydrocarbon addition at 1 atm and 298 K [3]. Solid lines indicate mixtures investigated in this study.

Acetylene (C_2H_2) was only found to be present in very small amounts (less than 1% for both blends) and was predicted to have almost no noticeable effect. While ethylene (C_2H_4) was predicted to have a significant effect for bio-syngas, it also makes up just over 5% of the mixture. There was almost no ethylene found to be present in coal syngas (around 0.1%), and as such it was predicted to have no discernable effect. The hydrocarbons chosen for further study were the ones predicted to have the most-significant impact on the laminar flame speed for both blends. A detailed breakdown of the resulting mixtures tested in the present study is shown in Table 1.

Table 1. Syngas mixtures with HC impurities

Mixtures Investigated (Mole Fraction)				
Mixture	H_2	CO	CH_4	C_2H_6
Coal-Neat	0.400	0.600	--	--
Coal-1.6% CH_4	0.3936	0.5904	0.016	--
Coal - 7.4% CH_4	0.3704	0.5556	0.074	--
Coal – 1.7% C_2H_6	0.3932	0.5898	--	0.017
Bio-Neat	0.500	0.500	--	--
Bio-5% CH_4	0.475	0.475	0.050	--
Bio-15% CH_4	0.425	0.425	0.150	--
Bio-0.8% C_2H_6	0.496	0.496	--	0.008

As seen in Table 1, the two hydrocarbons investigated in this study were methane and ethane. Methane was investigated at the high and low extremes found to be present in syngas mixtures. The maximum concentrations of methane found in typical syngas mixtures were 7.4% for the coal-derived syngas and 15% for bio-syngas. The minimum levels of methane were 1.6% for coal syngas and 5% for bio-syngas. Model predictions showed that the maximum percentage of methane, in both cases, would have a significant impact on the flame speed [3]. Ethane was chosen not because it comprised a

large percentage of the fuel, 0.8% for bio-syngas and 1.7% for coal syngas, but because of the significant reduction in flame speed predicted by the model.

4. EXPERIMENTAL SETUP

4.1 Vessel Design

Experiments were conducted in the high-pressure, high-temperature, stainless steel, constant-volume bomb at Texas A&M University shown in Figure 3. The design of this vessel is explained in detail in Krejci et al. [15]. The internal dimensions of the vessel are a 31.8 cm diameter and a length of 28 cm. Flames can be measured under near-constant-pressure conditions to a diameter of 12.7 cm.

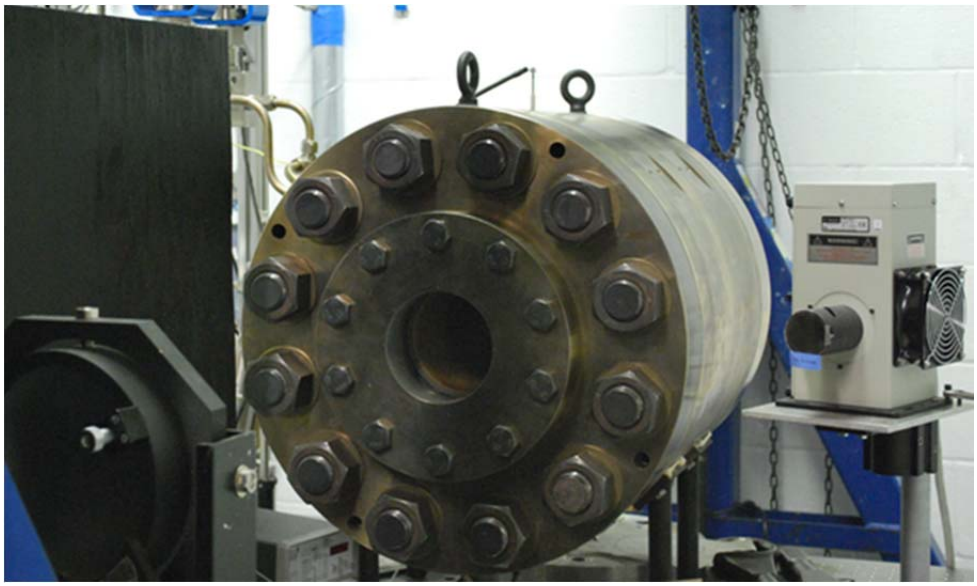

Figure 3. High-temperature high-pressure stainless steel constant-volume bomb. Light source and one parabolic mirror are visible. Fill and vacuum lines are visible entering vessel from upper left. Blast wall is to the right in the picture.

Prior to the syngas experiments, the electrode setup in the vessel was modified. This schematic highlighting this change is shown in Figure 4. It was noticed in previous

tests that once every five to ten experiments the spark would jump inside the electrode bore, causing the flame to burn down from the top when looking at the images. It was determined that this secondary flame was due to trapped gas in the igniter feed tube being ignited by the spurious spark event. The electrodes were modified to be mounted to the inner surface of the vessel as opposed to the outer surface, thus preventing any gas mixture from entering the igniter feed annulus. While the electrode insulation could still fail, and the spark could still jump to the wall of the vessel, there will no longer be any trapped gas mixture that might inadvertently ignite.

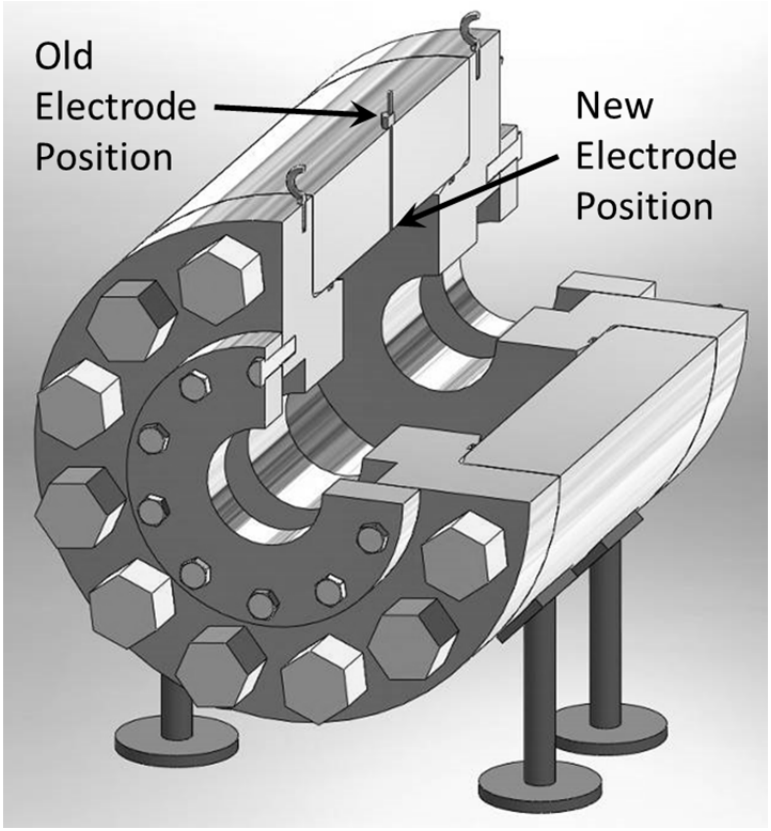

Figure 4. Cutaway view of HTHP vessel taken from Krejci [16]. Notice the change in electrode placement. Only the top electrode is shown.

4.2 Gaseous Mixtures

All mixtures were made using the partial pressure method via a 0-1000 Torr pressure transducer, and the experiments were conducted at room temperature (296 K ± 2 K). Research grade (99.5% pure) methane, ethane, hydrogen, carbon monoxide as well as ultra-high purity (99.999%) oxygen and nitrogen were used. For the low-methane coal syngas and the ethane mixtures, the respective hydrocarbon and hydrogen were premixed in a separate mix tank prior to being added to the vessel. This extra procedure was due to the very low partial pressure required for the minor hydrocarbon consituent. All other components were added individually. The carbon monoxide was stored in an aluminum cylinder and in a separate gas cabinet at below atmospheric pressure for safety reasons. As the line that the CO ran through from the safety cabinet to the manifold was quite long, CO detectors were placed at either end to detect any possible leak. These detectors were checked regularly. Also, all personnel working in the laboratory area were made aware whenever the CO bottle was opened and closed. Pictures of the manifold and the CO safety cabinet are in Figure 5.

Figure 5. Left: gaseous manifold, against blast wall to test cell. Right: CO safety cabinet; CO ran from cabinet into the manifold connecting at the circular valve (center one of the five visible in picture).

4.3 Experimental Procedure

Each gaseous mixture was ignited by a central spark ignition system. Experimental data were collected using a high-speed camera (Photron Fastcam SA1.1) and a Z-type schlieren setup, shown in Figure 6. While the camera captured images through complete combustion, only images from ignition until the flame reached the edge of the window were used for analysis. Frame rates used for this data set ranged from 3,000 to 18,000 fps. This wide range of frame rates was used due to the range of predicted flame speeds, from 20 cm/s to 200 cm/s. Ideally between 100 and 200 frames would be available for analysis. The adjustment of the frame rate allowed the program to process the data without having too little or way too much data to analyze.

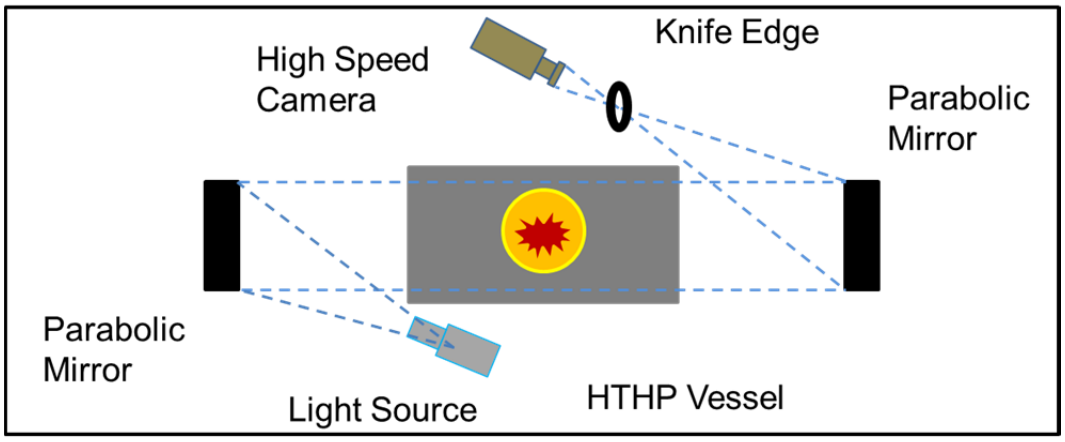

Figure 6. Z-type schlieren setup currently in use in the laboratory. Schematic shown is not drawn to scale.

Images were processed using an internally developed MATLAB-based edge detection program. The circle fitting edge detection is shown in Figure 7. The raw output of the image analysis gives the burned stretched flame speed, S_b. This is also sometimes shown the change in radius with respect to time or, dr_f/dt. The unburned, unstretched flame speed and burned-gas Markstein length were calculated using the appropriate nonlinear method as outlined by Chen [17].

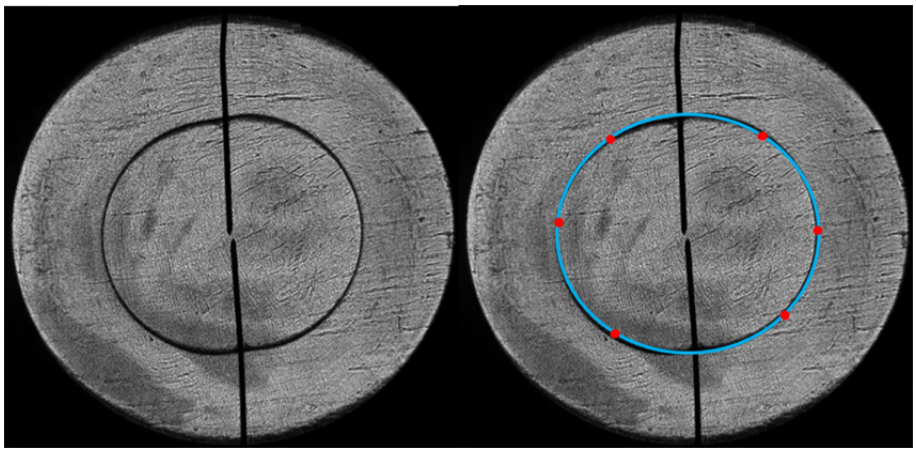

Figure 7. Sample of raw image and six-point circle fit MATLAB edge detection analysis used to determine S_b.

Non-linear method I:
$$S_b = S_b^0 - S_b^0 L_b \left(\frac{2}{r_f}\right) \tag{3.1}$$

Non-linear method II:
$$LN(S_b) = LN(S_b^0) - S_b^0 L_b \left(\frac{2}{r_f S_b}\right) \tag{3.2}$$

The method shown in Eqn. 3.1 is used for flames with a positive Markstein lengths and the method shown in Eqn. 3.2 is used when the Markstein length is negative. (Markstein lengths are discussed in detail in Section 5.5, and it is shown that negative Markstein lengths were only seen for the leanest mixtures investigated.) The methods outlined above give the unstretched, burned flame speed, S_b^0. Flame stretch is defined in equation 3.3, while flame curvature which actually appears in both non-linear methods is defined as $2/r_f$.

$$\kappa = \frac{2}{r_f} S_b \tag{3.3}$$

Another step is required to determine the unburned unstretched flame speed, S_L^0. This flame speed is simply obtained by dividing the unstretched, burned flame speed by the density ratio, σ. This calculation is shown in Eqns. 3.4 and 3.5.

$$\sigma = \frac{\rho_u}{\rho_b} \tag{3.4}$$

$$S_{L,u}^0 = \frac{S_b^0}{\sigma} \tag{3.5}$$

To accurately determine the laminar flame speed, both wall and ignition effects need to be taken into account. This compensation is done by removing them from the calculation and is manually done during the analysis of S_b. As can be seen in Figure 8 and Figure 9, the slope of S_b versus Stretch, significantly changes with wall effects on the left and ignition effects on the right. Images are removed until the slope remains relatively constant. When this point is reached there will also be minimal changes in $S^0_{L,u}$.

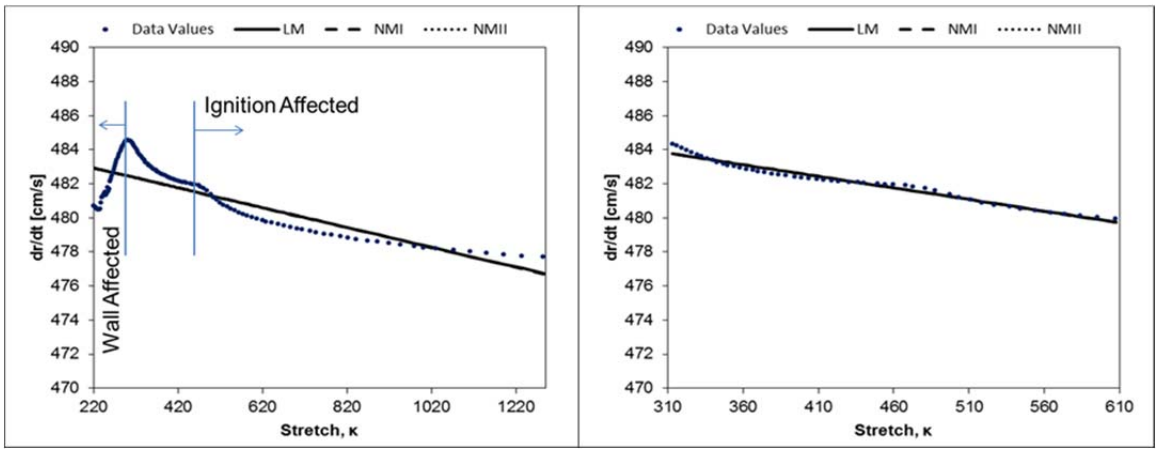

Figure 8. Sample burned gas flame speed vs. stretch plots used to remove wall and ignition affects for non-linear method 1, positive Markstein length. Plot on left is near the starting point where the effects are most visible. Plot on right shows the finishing point when noticeable effects have been removed.

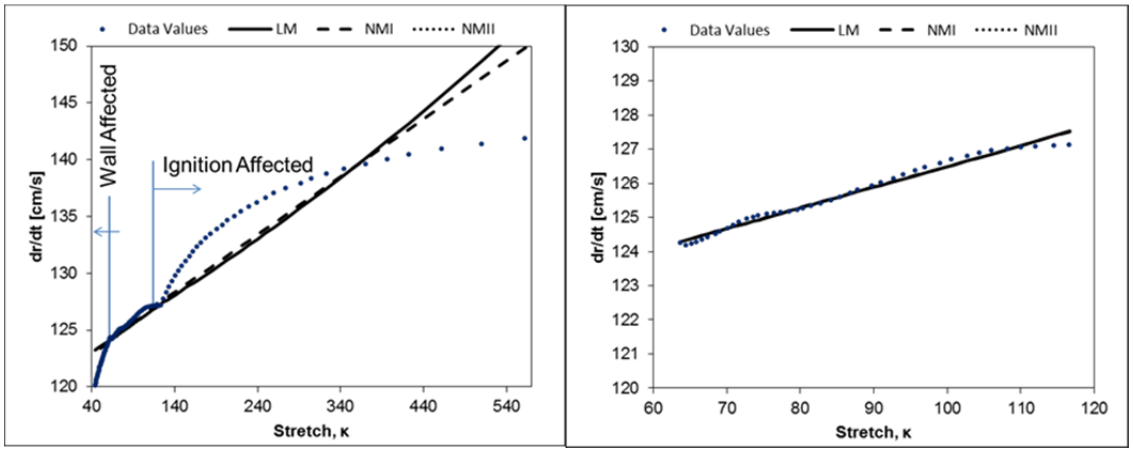

Figure 9. Sample burned gas flame speed vs. stretch plots used to remove wall and ignition affects for non-linear method II, negative Markstein Length. Plot on left is near the starting point when effects are most visible. Plot on right shows the finishing point when noticeable effects have been removed.

It is totally based on the judgment of the person analyzing the data when to stop removing points due to wall or ignition effects. It might seem that this manual method could increase uncertainty in the flame speed results. However, once wall and ignition effects are removed there is minimal difference in the output flame speed, putting any variation based on who analyzed the data well within the experimental uncertainty discussed below in Section 4.5.

4.4 Chemical Kinetic Model

The laminar flame speeds in this work have been simulated using AramcoMech 1.3 [18], which was developed to describe the oxidation of small hydrocarbon and oxygenated hydrocarbon species, C0 to C5. The complete mechanism is 1805 reactions and 316 species. As in the numerical study presented in Mathieu et al. [3], the high-temperature version of the mechanism consisting of 1273 reactions and 188 species, was used. The simulations were performed using the Premix code of Chemkin Pro. To reduce the computational cost, mixture-averaged transport equations were utilized. Thermal diffusive effects were also included. For all calculations, the GRAD and CURV values were both set to 0.01, and an average of 1000 grid points was utilized. The solutions were shown to be grid independent at this resolution.

5. RESULTS

5.1 Neat Mixtures

As seen in Figure 10, the experimental results for the neat mixtures of CO and H_2 match the model predictions very well. As expected, the syngas mixture with the greater amount of hydrogen, i.e. the bio-syngas, produced a flame speed that was on average 20.8 cm/s faster than the coal syngas mixture. Both mixtures saw a peak in flame speed around an equivalence ratio of 2.0. The experimental data for both mixtures stayed very close to the model with differences typically between about 1 and 2 cm/s.

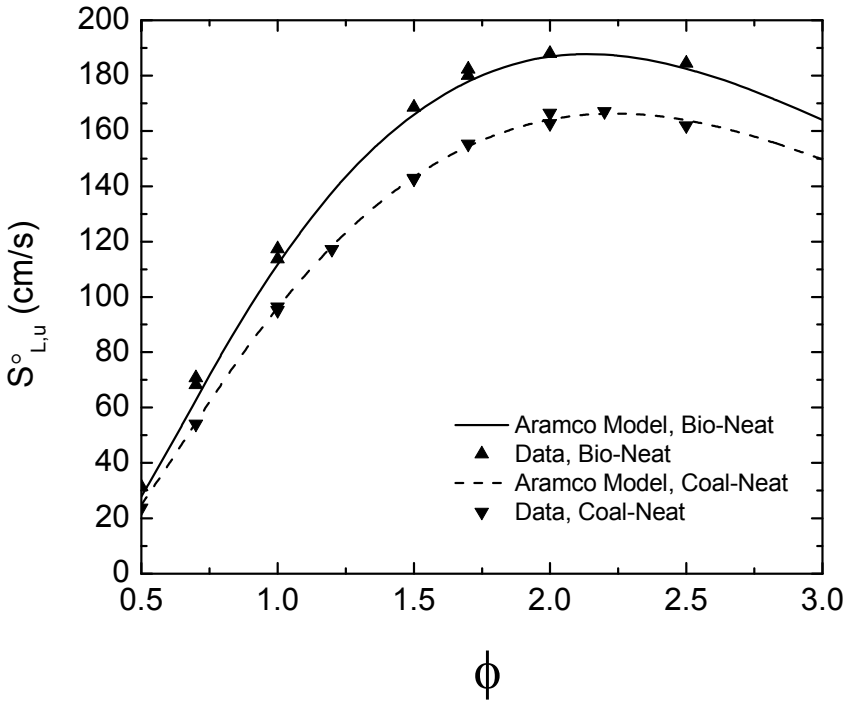

Figure 10. Laminar flame speeds for the baseline bio-syngas and coal syngas mixtures (Bio-neat and Coal neat) at 1 atm and 296 K.

5.2 Coal Syngas Blends

As expected, the addition of hydrocarbons to the coal syngas reduced the flame speed. Figure 11 shows the model predictions and the experimental results for these syngas blends. The model predicts well the shape of the flame speed curve and predicts the peak flame speed at the correct equivalence ratio. However, the model under predicts the flame speed for all of the mixtures when hydrocarbons are added. This under prediction is most noticeable at rich mixtures when the model curves deviate from each other, and the effects of the hydrocarbons are more noticeable. On average, the low-methane-concentration (1.6%) model under predicts the flame speed by 2.1%. The next model, with ethane (1.7%), under predicts the flame speed by 10.8%. The greatest difference was with the highest methane concentration (7.4%), which demonstrated a 17.4% average under prediction of the model. As expected, the greater percentage of hydrocarbons added to the syngas blend the greater reduction in the laminar flame speed. While the low-methane and the ethane mixtures had nearly the same concentration of hydrocarbon addition, 1.6% to 1.7% respectively, the effect of the ethane is noticeably greater.

The uncertainty of the experiments is discussed at length in Section 4.5. Calculated uncertainty for the coal syngas mixtures ranged from 5.8 cm/s to 6.3 cm/s, with an average of 6 cm/s. One representative error bar per curve is shown, the rest have been removed for clarity.

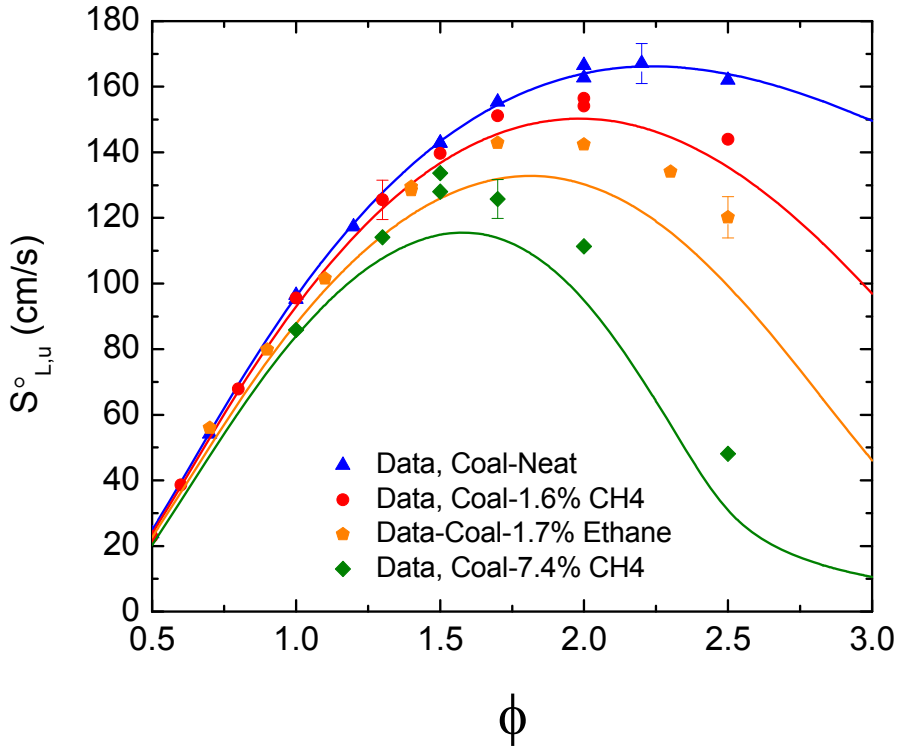

Figure 11. Laminar flame speeds for coal syngas blends with and without hydrocarbons at 1 atm and 296 K. Symbols are data; lines are model predictions.

5.3 Bio-Syngas Blends

Like the coal syngas blends in Figure 11, the bio-syngas blends also saw a reduction of flame speed with the addition of hydrocarbons. Also like the coal-derived blends, the peak flame speed for the bio-syngas shifted toward an equivalence ratio of 1 as more hydrocarbons were added. The experimental results are plotted in comparison to the model predictions in Figure 12. For the bio-syngas case, ethane was added in the very small amount of 0.8%. Even in this small amount, it had a significant impact on the

flame speed, with a reduction of 11.5 cm/s near the peak equivalence ratio. The model under predicted the flame speed by an average of 7.7%. The low- methane case (5%) saw a reduction in peak flame speed of 34.8 cm/s, with the peak equivalence ratio shifting from φ = 2.1 to 1.7. In general the model under predicts the flame speed by an average of 12.8%. This trend continues for the high-methane case (15%). Here the peak flame speed of 108.2 cm/s was found at φ = 1.3. The model under prediction averages 15.9% for this mixture. Uncertainty for the bio-syngas mixtures ranged from 5.8 cm/s to 6.7 cm/s, with an average of 6 cm/s. Only one error bar per curve is shown.

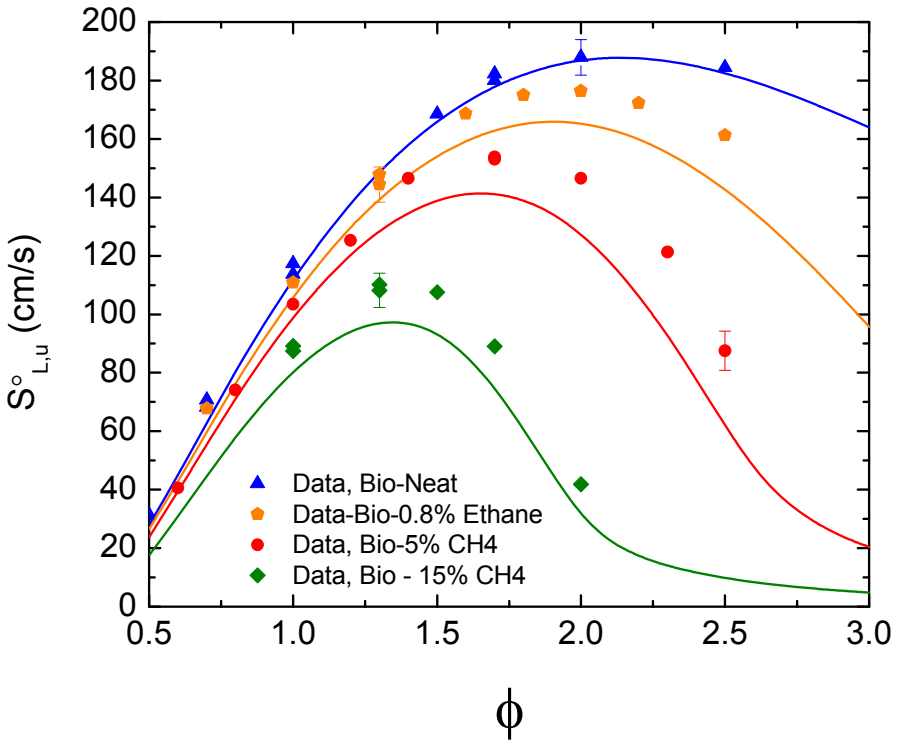

Figure 12. Laminar flame speeds for bio-syngas blends with and without hydrocarbons at 1 atm and 296 K. Symbols are data; lines are model predictions.

5.4 Uncertainty Analysis

As with all experimental procedures determining uncertainty in measurements is very important. It is known that the absolute uncertainty is high for high-hydrogen-content flames, mainly because the nominal flame speeds are the highest for H_2-based flames. In the work of Krejci et al. [15], the uncertainty of pure-hydrogen flames was found to be on average 7.1 cm/s from φ = 0.5 to 5. This value can be tentatively used as the worst-case uncertainty for the syngas flames. This upper limit assumes that the addition of the hydrocarbon will reduce the uncertainty. This expectation is reasonable because the uncertainty of methane is estimated to be around 0.27 cm/s according to Ravi et al. [19].

A more-accurate uncertainty was calculated for the syngas mixtures using the Kline and McClintock method as outlined by Moffat [20] and used in [19] and [15]. The total uncertainty, U_{SL}, is a combination of the bias error, B_{SL}, and the random error, P_{SL}.

$$U_{SL} = (B_{SL}^2 + P_{SL}^2)^{0.5} \tag{5.1}$$

Bias uncertainty is based off of inherent differences in the experiments. There are known precisions tied to both the pressure and temperature gauges used, leading to uncertainty in the partial pressures, and thus the equivalence ratio, and the temperature of the experiment. These uncertainties were taken from the manufacture provided specifications. To determine how changes in temperature and equivalence ratio affect the flame speed, the relationship shown in equation 5.2 was used. The kinetic model

was then run at increasing temperatures, of 350, 400, and 450 K, to determine a surface fit to the equation. While the experiments show that the model is not perfect, it still is useful to determine how much impact small differences in temperature and equivalence ratio have on flame speed.

$$S_{L,u}^{0} = (a + b\varphi + c\varphi^{2} + d\varphi^{3} + e\varphi^{4})\left(\frac{T}{298}\right)^{(p+q\varphi+r\varphi^{2}+s\varphi^{3})} \quad (5.2)$$

The coefficients to the equation were determined using the surface-fitting tool in MATLAB. The calculated coefficients are listed tin Table 2. From the results in that table, the bias uncertainty was calculated using Eqn. 5.3.

Table 2. Coefficients of flame speed equation (Eqn. 5.2) for mixtures investigated.

Mixture	a	b	c	d	e	p	q	r	s
Coal- Neat	-56.98	167.70	6.62	-26.09	4.31	2.42	-1.07	0.40	-0.04
Coal-1.6% CH_4	-49.84	142.8	30.49	-36.27	5.25	2.35	-0.87	0.21	0.02
Coal-7.4% CH_4	-17.20	-11.49	247.90	-161.40	27.04	3.37	-3.10	1.55	-0.18
Coal-1.7% C_2H_6	-32.07	77.36	102.00	-70.66	10.35	2.48	-1.05	0.20	0.05
Bio-Neat	-71.77	206.00	4.26	-32.25	5.57	2.42	-1.02	0.35	-0.30
Bio-5% CH_4	-9.796	-41.43	302	-181	28.64	3.30	-2.55	0.98	-0.04
Bio-15% CH_4	-137.3	419.8	-223.20	20.54	4.39	1.21	-0.85	1.85	-0.63
Bio-0.8% C_2H_6	-55.75	153.3	51.75	-51.97	7.79	2.45	-1.04	0.27	0.01

$$B_{SL} = \sqrt{\sum_{i=1}^{n} \left(\frac{\partial S_{L,u}^{0}(x_i)}{\partial x_i} u_i \right)^2} \tag{5.3}$$

The random uncertainty, P_{SL}, was calculated based off of the 13 repeated points throughout the whole data set. There were between one and three repeated points on each of the eight curves investigated. From the repeated points, the average difference in flame speed was calculated to be 2.3 cm/s with a standard deviation of 1.5 cm/s. P_{SL} was estimated using the following equation.

$$P_{SL} = \overline{X}_{dif} + 2.25 SD_{dif} \tag{5.4}$$

This method allowed for the total uncertainty to cover the spread seen in the data. The overall average estimated uncertainty for the data is 6.0 cm/s.

In this data set, most of the uncertainty came in the form of random error. The uncertainty model showed very little change due to slight differences in temperature or equivalence ratio, except at very rich conditions.

6. DISCUSSION

6.1 Equivalence Ratios

Equivalence ratio is normally used as a parameter in flame speed experiments. It is traditionally defined as the fuel-to-oxygen ratio of the mixture divided by the stoichiometric fuel-to-oxygen ratio.

$$\varphi = \frac{{}^{N_f}\!/_{N_{Ox}}}{({}^{N_f}\!/_{N_{Ox}})_{ST}} \tag{6.1}$$

It is the base equation for determining how lean or rich a mixture is. Some recent studies have suggested that it is not always the ideal parameter to use when analyzing experimental results. These adjustments on the equivalence ratio are discussed below. The data are graphically presented using these modified equivalence ratios; however, for the model comparison in Section 6.2, the traditional definition will be used.

6.1.1 Oxygen Equivalence Ratio

It has been proposed by Mueller [21] that the traditional definition of equivalence ratio is an inaccurate parameter when the fuel contains oxygen. This view is because the oxygen in the fuel, for the syngas it is the CO, is treated as part of the fuel and not as part of the oxidizer. The proposed method contained therein uses the oxygen equivalence ratio, φ_Ω, as a more-accurate portrayal of the actual stoichiometry of the fuel-to-oxidizer mixture. This method treats the CO fraction of the fuel, correctly, by treating it as

already being partially oxidized. Calculating φ_Ω is a two-step process. First the oxygen ratio, Ω, shown in equation 6.2 is needed. The oxygen ratio is defined as the ratio of oxygen atoms to the stoichiometric number of oxygen atoms for the given mixture.

$$\Omega = \frac{N_O}{N_{O,ST}} \tag{6.2}$$

$$\varphi_\Omega = \frac{1}{\Omega} \tag{6.3}$$

As seen in equation 6.3, the oxygen equivalence ratio is the inverse of the oxygen ratio. A comparison of the two equivalence ratios is shown in Figure 13. As can be seen, φ_Ω is slightly higher than φ for lean mixtures and significantly lower for rich mixtures. At the stoichiometric condition, both φ and φ_Ω are equal to one. If this method were applied to a pure hydrocarbon, it would result in the normal equivalence ratio, φ.

Figure 14 shows the experimental data plotted using the oxygen equivalence ratio. While this is a useful adjustment when comparing partially oxidized fuels, such as syngas, to more traditional fuels, all of the syngas blends experience roughly the same adjustment. Since they all shifted together, it is debatable whether or not this is necessarily a useful method in this case since no useful information is obtained other than to shift the peaks to a leaner effective equivalence ratio.

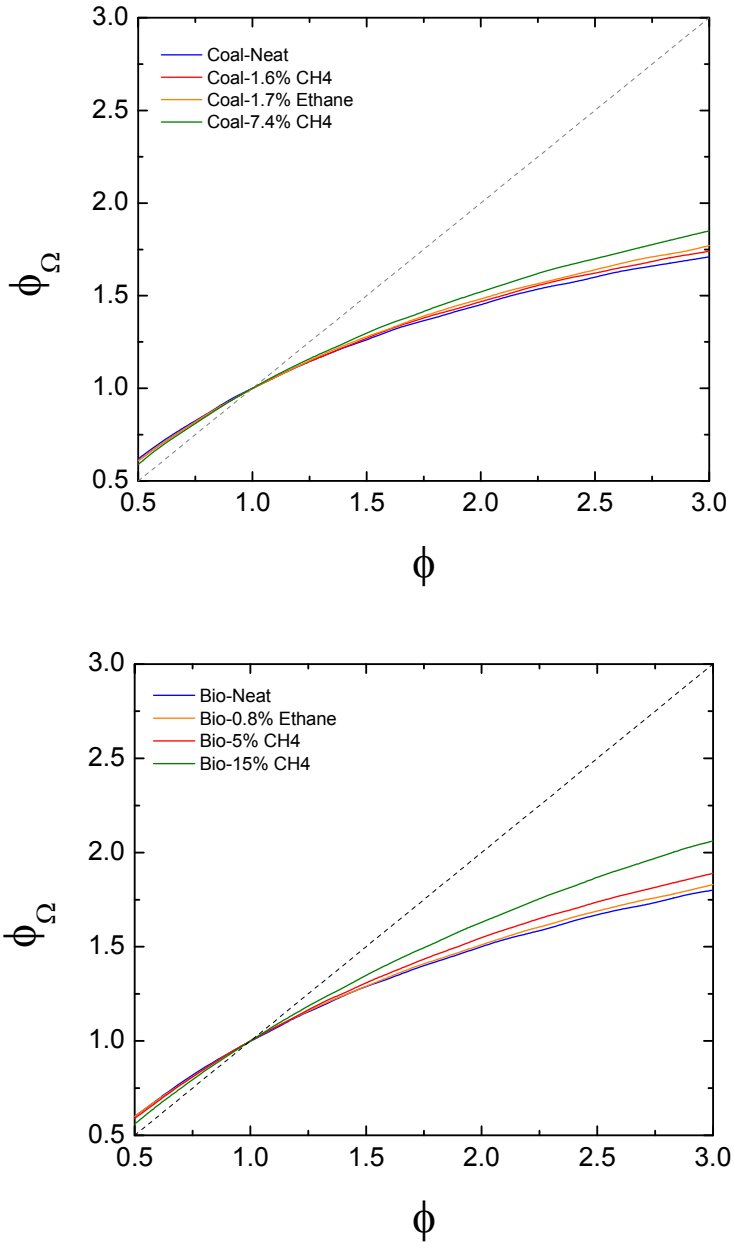

Figure 13. Oxygen equivalence ratio compared to the regular equivalence ratio for bio and coal syngas blends

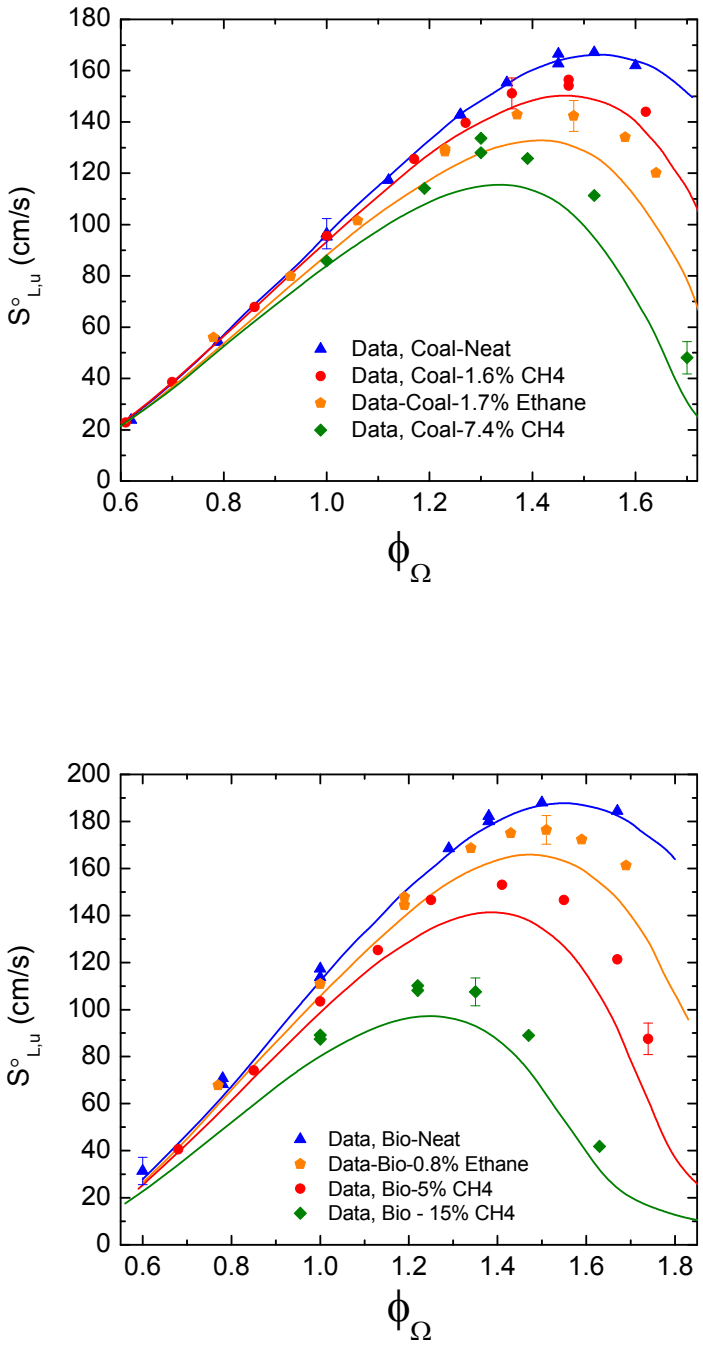

Figure 14. Experimental data and model predictions plotted against oxygen equivalence ratio for coal and bio syngas blends.

6.1.2 Normalized Equivalence Ratio

A recent work by Law et al. [22] proposed the use of a normalized equivalence ratio, $\bar{\varphi}$, to show the even distribution of experimental scatter on flame speed plots. Due to the nature of flame speed curves, with a steep climb on the lean-mixture side, it can appear that there is less scatter in measurements. This graphical appearance is due to lean mixtures being limited between φ equal to zero and one, while the rich mixtures occupy most of the graph going from one to the highest level investigated, in the case of this study it is 3. This graphical representation could be misleading especially when very rich mixtures are investigated. The proposed, normalized equivalence ratio is shown in Eqn. 6.4.

$$\bar{\varphi} = \frac{\varphi}{(1+\varphi)} \tag{6.4}$$

This method results in the normalized equivalence ratio always being less than one. This limitation causes the scatter to appear more evenly dispersed for both lean and rich mixtures. While this method might visually make the scatter appear similar for both lean and rich mixtures, any mathematical analysis of the scatter would show this.

The data for both syngas blends are plotted vs the model using the normalized equivalence ratio in Figure 15. There is little change in the data scatter, with the most noticeable change being the appearance of the model prediction curve.

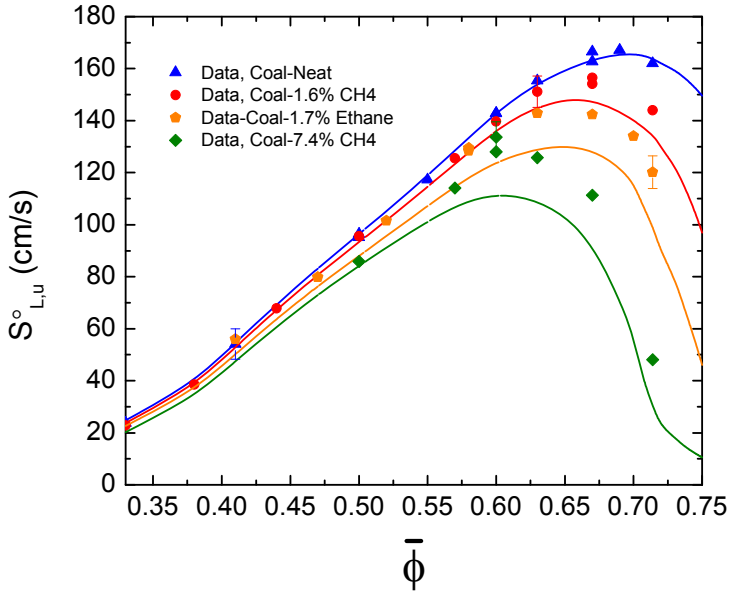

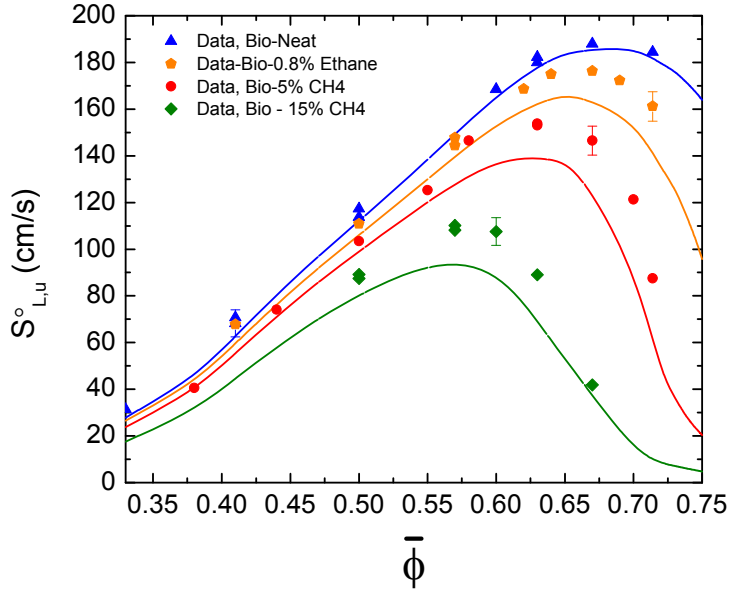

Figure 15. Experimental data and model predictions plotted against the normalized equivalence ratio for coal and bio syngas blends.

6.2 Model Comparison

Overall, the experimental results agree well with the model predictions. This conclusion is especially true for both neat mixtures. However, this excellent agreement ends when methane or ethane were added. Generally the model remains very good for lean mixtures. The disagreement is seen mostly for rich mixtures. The data follow the general shape of the curve predictions, and the peak flame speeds are at the predicted equivalence ratios. However, the model consistently predicts a slower flame speed than the data.

While this tendency has been shown for the syngas mixtures investigated in this study, it is important to show that the current model is very accurate at extreme ends of the spectrum in terms of hydrogen at the high end and methane at the lower end. Figure 16a shows the model predictions compared to previous experimental data from the author's group [15, 23] for pure hydrogen and methane flames in addition to the coal syngas results from the present work. As can be seen, the model does very well with pure hydrogen, the neat syngas, and pure methane. The only noticeable disagreement is in the middle flame speed region when hydrocarbons are added to the syngas blend.

Comparing syngas blends to pure hydrogen and methane is an appropriate time to use the oxygen equivalence ratio, discussed earlier. Figure 16b shows the full model comparison using φ_Ω, as opposed to Figure 16a which used φ. As can be seen, different conclusions could be drawn depending on which equivalence ratio is used. Under the traditional definition of φ, the syngas curves tend to follow more closely the shape the pure methane curve. When using φ_Ω, the syngas curves look similar to the hydrogen curve, noticeable by the steep increase in flame speed.

6.3 Flame Speed Sensitivity Analysis

The chemical kinetics play an important part in the calculation of the flame speed, and to this end, the National University of Ireland at Galway conducted a flame speed sensitivity analysis to determine the important reactions that dominate the flame speed and control the changes in the chemistry [24]. The results of this analysis are summarized here for completeness in Figure 17 through Figure 19. A brief discussion of the results follows.

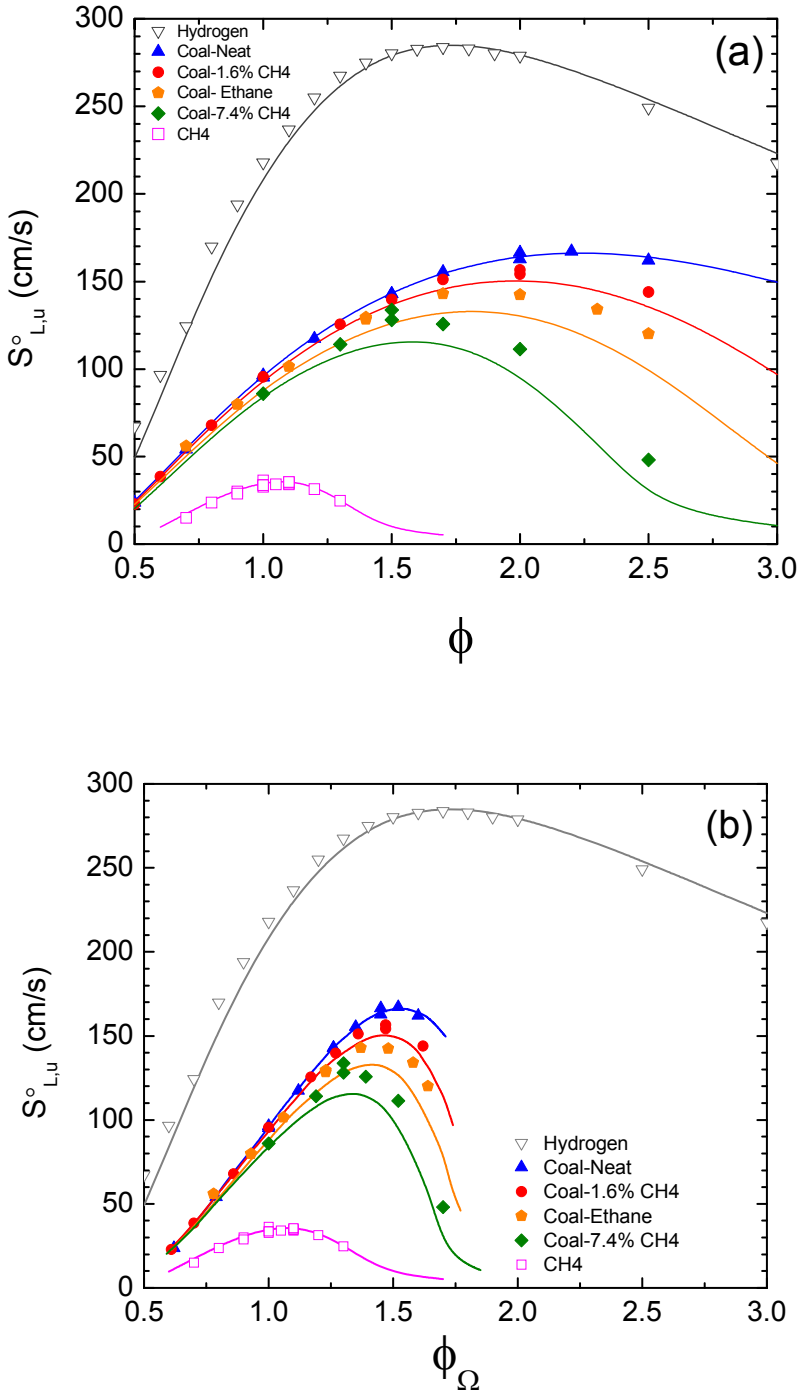

Figure 16. Laminar flame speed calculations for hydrogen (gray) and methane (pink) compared to the results of coal syngas in the current study (a) equivalence ratio, (b) oxygen equivalence ratio. Symbols are data; lines are model predictions.

The sensitivity analysis was only conducted for the coal syngas mixtures. For each mixture three equivalence ratios, a lean φ=0.7, a slightly rich φ=1.4, and a very rich φ = 2.1 were investigated. This range of mixtures insured any effect of equivalence ratio on key reactions would be captured in the analysis. The reactions found to be most important are shown in Table 3.

Table 3. Key chemical reactions for coal syngas blends

Number	Reaction
R1	$CO + OH \leftrightarrow CO_2 + H$
R2	$H + O_2 \leftrightarrow O + OH$
R3	$HO_2 + H \leftrightarrow OH + OH$
R4	$H + O_2 (+M) \leftrightarrow HO_2 (+M)$
R5	$H + OH + M \leftrightarrow H_2O + M$
R6	$HO_2 + OH \leftrightarrow H_2O + O_2$
R7	$CH_3 + H (+M) \leftrightarrow CH_4 (+M)$
R8	$CH_3 + O \leftrightarrow CH_2O + H$
R9	$HCO + M \leftrightarrow CO + H + M$
R10	$C_2H_5 + H \leftrightarrow CH_3 + CH_3$

The results of the neat mixture are shown in Figure 17. The most sensitive reaction for all equivalence ratios shown is R1. However, its sensitivity coefficient decreases as the mixture becomes richer. In contrast, the sensitivity coefficient of R2 increases at richer mixtures, becoming almost equal to that of R1 at φ = 2.1. The largest change in sensitivity is seen in R4 which goes from a negative sensitivity, decreasing the

flame speed, at lean conditions to a positive sensitivity, and therefore increasing the flame speed, at rich conditions. This increase is due to R4 competing with the terminating reactions of R5 and R6.

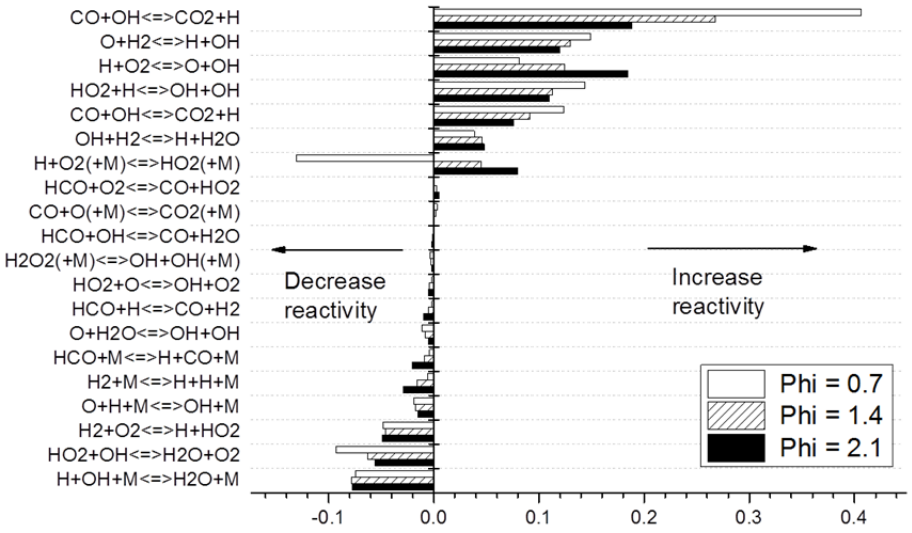

Figure 17. Flow rate sensitivity analyses of laminar flame speeds for coal-neat syngas Initial conditions 1.0 atm, 296 K, φ = 0.7, 1.4, and 2.1 [24].

When CH_4 is added significant changes are visible in the sensitivity analysis. These changes become more apparent as more methane is added. Figure 18a shows the analysis for 1.6% CH_4, while Figure 18b is for 7.4% CH_4. For both cases, the most-sensitive reaction remains R1 for lean mixtures. Like it did for the neat mixture, R2

continues to become more sensitive as the mixture becomes richer. This influence of R2 becomes more pronounced as more methane is added. This increase in importance is due to competition with R7 as more CH_4 is added to the mixture. While R7 is only slightly decreasing reactivity for the low CH_4 blend, its role is more visible for the high-methane blend. Also becoming more important as more CH_4 is added is R8. Like R2, this reaction becomes more reactive as φ increases. This increased reactivity is due to it being a major consumption pathway for CH_3 radicles at rich conditions. Reaction R9 has a slightly negative reactivity coefficient at the 1.6% CH_4 mixture, but as more CH_4 is added the reactivity coefficient becomes positive. This change in direction is due to the consumption of the CH_3 radicles through R8, causing it to be more reactive.

At higher equivalence ratios, R2 is limited by the lower concentration of O_2, and competition from R7. At the richest conditions, these two reactions dominate, as shown in Figure 18b for the 7.4% CH_4 mixture. This competition causes the sharp reduction in flame speed predicted by the model and seen in the experimental data. The negative effect of adding CH_4 to the mixture clearly dominates the flame speed.

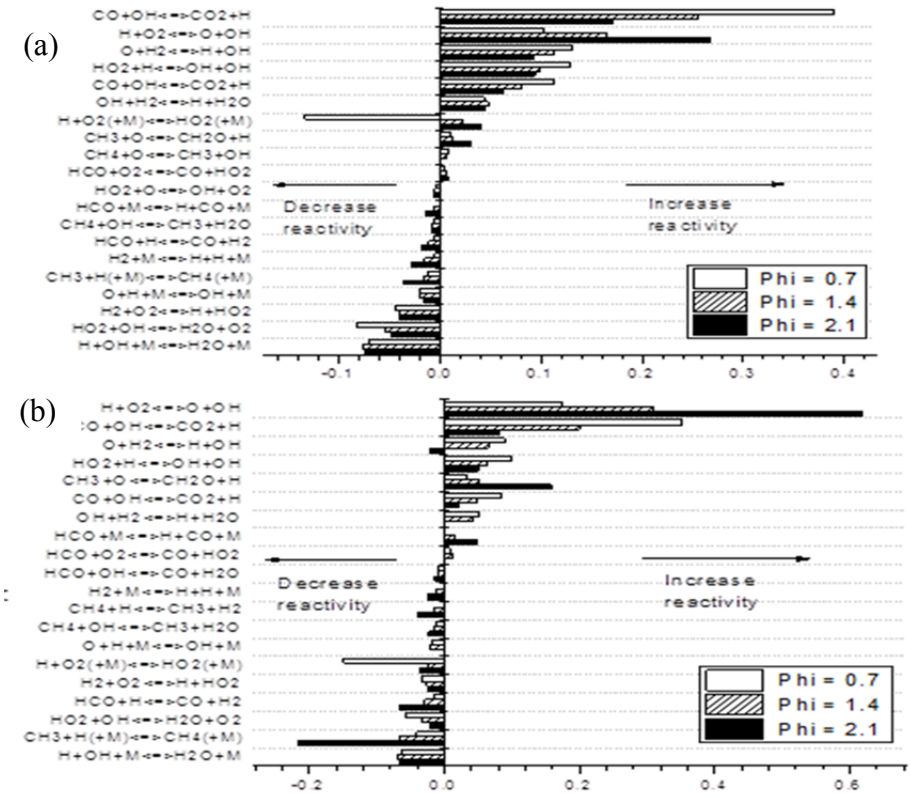

Figure 18. Flow rate sensitivity analyses of laminar flame speeds for coal syngas with CH_4 addition. (a) 1.6%, (b) 7.4%. Initial conditions 1.0 atm, 296 K, φ = 0.7, 1.4, and 2.1 [24].

The addition of C_2H_6 is shown if Figure 19, and the negative effect it has on the flame speed is seen. However, this is mostly due to the C1 chemistry through R7, as the C2 chemistry appears to be of minor importance. This reduced important on C2 chemistry is due to the H-atom abstraction from the C_2H_6, causing the C_2H_5 to be easily converted to CH_3 via R10, which becomes a major consumption pathway, especially at rich conditions. This conversion of the ethyl causes the reactions leading to the formation of C_2H_5 to have a very minor contribution to the decrease in reactivity. The recombination of CH_3 and H atoms continues to be as important as it was with the CH_4

addition. Reaction R10, while only having a slightly negative reactivity coefficient, is the only one of the C2 chemistry reactions seen to have any change as the mixture became richer. It is also clearly seen that R7 is a much stronger in competitor for the H atoms, as seen in Figure 19. It should be noted that through R10, every C_2H_5 radical produces 2 CH_3 radicals to proceed through R7. This increased production of relatively unreactive methyl radicals causes the decrease in flame speed with the addition of C_2H_6.

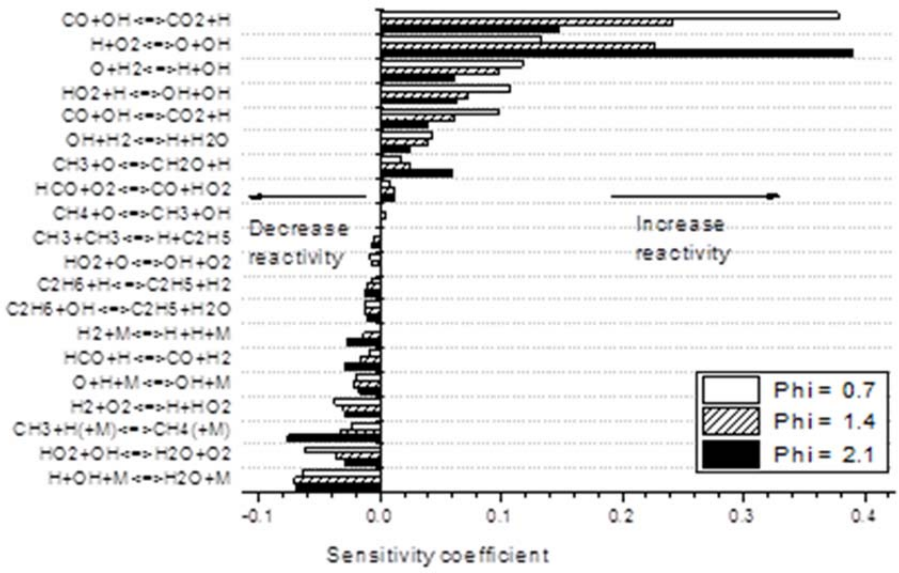

Figure 19. Flow rate sensitivity analyses of laminar flame speeds for coal syngas with 1.7% C_2H_6. Initial conditions 1.0 atm, 296 K, φ = 0.7, 1.4, and 2.1 [24].

As mentioned above the model did a very good job at predicting the flame speed for the neat mixtures, but under-predicted the flame speed when either CH_4 or C_2H_6 was

added. Refinement of the C1 and C2 chemistry in the mechanism is needed to better model the flame speed.

6.4 Radiation Effects

The effects of radiation on the flame speed can also be considered. Santner et al. [25] found the reduction in flame speed due to radiation heat loss from the flame to be small, on the order of a few percent. In the present results, the experimental data are consistently at faster flame speeds than the model predictions, indicating that if a radiation correction were included, the data would move further above (and away from) the predictions. Hence, possible radiation effects do not explain the current differences between data and model. For the present study, the effects of radiation are neglected.

6.5 Image Analysis

Image analysis of the growing flame showed two things. First, leaner mixtures tended to be less stable than richer mixtures, and second, hydrocarbon addition increased the stability of the flame. Figure 20 shows a small but representative selection of recorded images from a wide range of the data collected. These images are examples of trends seen throughout the data set. Note that the electrodes have been removed from the images to make the details of the flames easier to see.

The flame for the neat bio-syngas blend became unstable almost immediately. This flame is the leanest condition tested, making instability expected per the Markstein lengths and Lewis numbers for these mixtures (see below). Signs of a wrinkled flame are

visible in the first of the images shown. By the last images presented in Figure 20, the flame is very wrinkled, and no longer very spherical. The two coal syngas cases presented are very similar to each other. Both are flames near φ = 1, with the ethane addition being a slightly lean flame (φ = 0.9), and the neat case slightly rich (φ = 1.2). Both of these coal syngas flames are noticeably more stable than the lean bio-syngas. The neat coal flame begins to noticeably show instabilities in the second to last image shown. The coal flame with ethane although at a leaner condition (φ = 0.9) stays stable longer. There might be a slight hint of instabilities beginning in the last of the ethane coal images. The bio-syngas blend with 15% methane is the most stable. The flame stays nearly perfectly spherical throughout the images presented, with no hint of instabilities beginning. Note that the present data for un-stretched, unburned laminar flame speed were derived from the data using a method that determines numerically when the occurrence of instabilities begins to influence (i.e. accelerate) the flame propagation. Therefore, the S_L° data herein do not contain the effects of the instabilities. Further details on this data reduction procedure can be found in Lowry et al. [23].

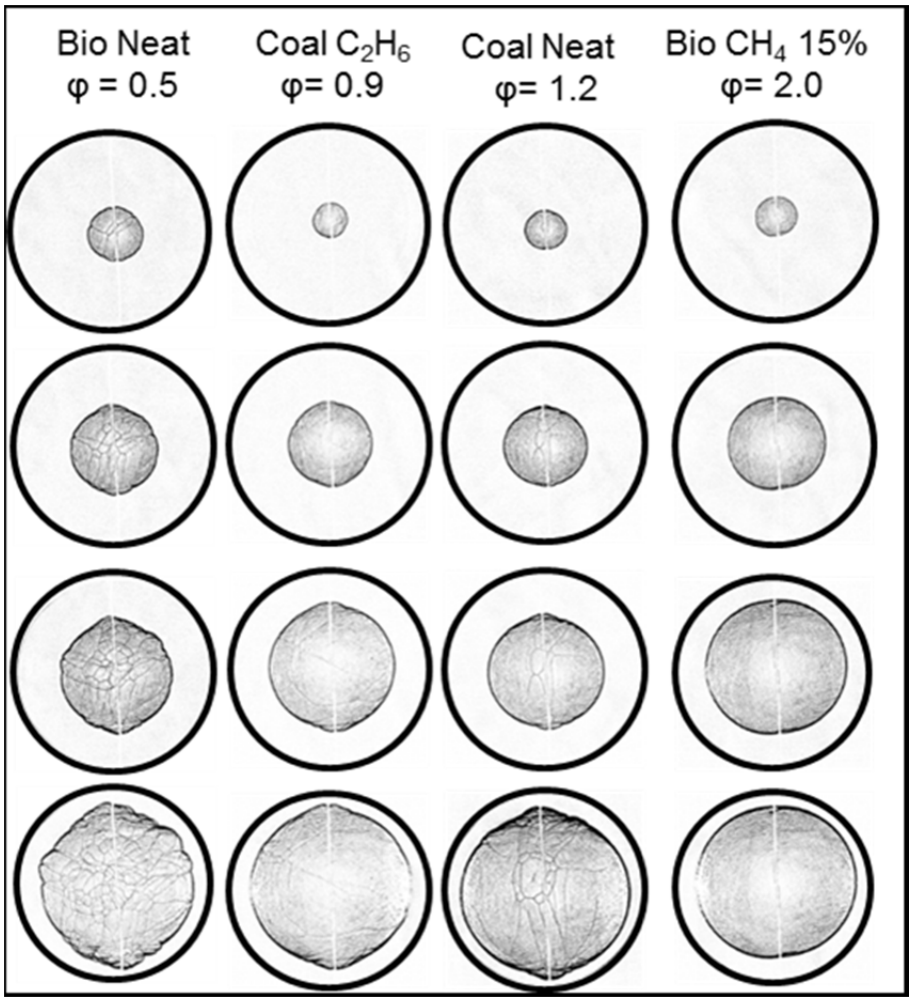

Figure 20. Sample flame images for four different syngas blends at different equivalence ratios. Time increases in each column from top to bottom.

6.6 Markstein Length

The Markstein length is typically presented as one of the key parameters of flame speed as it is a very good indication of the stability of the flame. It can also be thought of as the response of the flame speed to the strain rate as defined by Burke et al. [26]. As described by Monteiro et al. [12], the Markstein Length is the slope of the S_b versus stretch plot.

It is also pointed out that positive Markstein lengths mean the flame speed decreases with the increase of stretch, while a negative Markstein length means the flame speed increases with stretch. This dependence of stretch on Markstein length means when there is a negative Markstein length any instability in the flame will grow. This trend was seen in the image analysis presented above, where the images for lean mixtures, which happened to have negative Markstein lengths, were less stable.

The Markstein lengths for the coal syngas blends showed good agreement across all blends and equivalence ratios investigated. As can be seen in Figure 21, the Markstein length averaged around 0.05 cm for all mixtures investigated. The only significant deviations from this value range were at the leanest and richest equivalence ratios investigated. Negative Markstein lengths were calculated for the neat mixture at φ = 0.5 and 0.7, and for the low-methane mixture at φ = 0.5 and 0.6. The methane added in the lower case significantly increased the Markstein length and moved the flame closer to being stable. For the high-methane mixture at φ=2.5, which was the richest case investigated, the Markstein length increased to 0.22 cm.

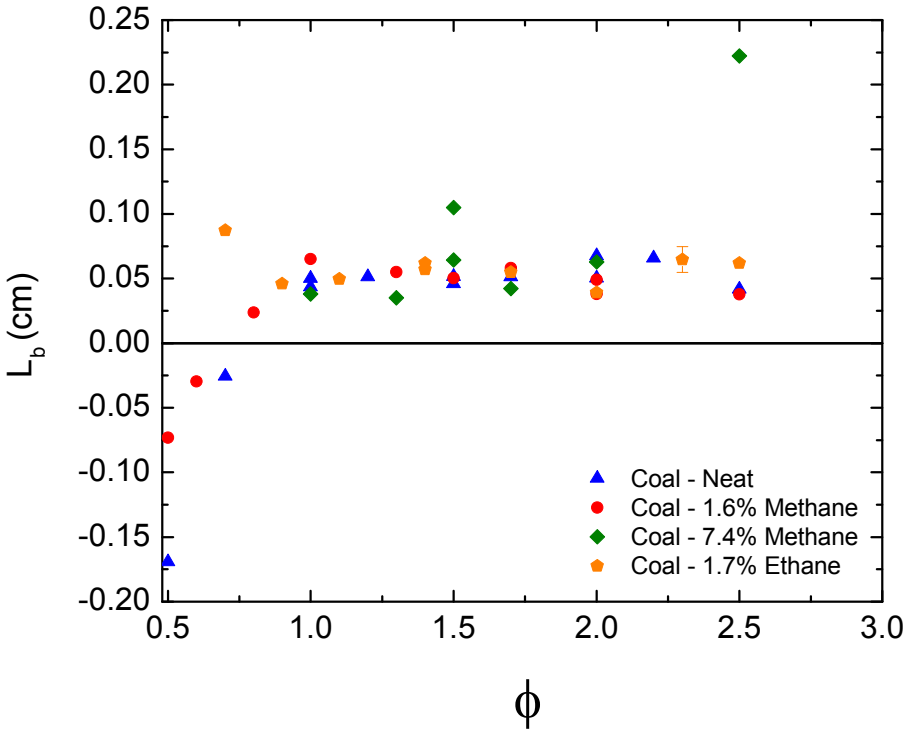

Figure 21. Burned-gas Markstein lengths for coal syngas blends with and without hydrocarbon addition to the baseline mixture at 1 atm and initial temperature of 296 K.

The Markstein lengths for the bio-syngas mixtures investigated showed similar trends. Over a majority of the equivalence ratios investigated, all mixtures had an average Markstein length just over 0.06 cm. As can be seen in Figure 22, the greatest variance was at the leanest and richest equivalence ratios. Like the coal syngas blend, the high-methane mixture returned a relatively large Markstein length for the richest case investigated.

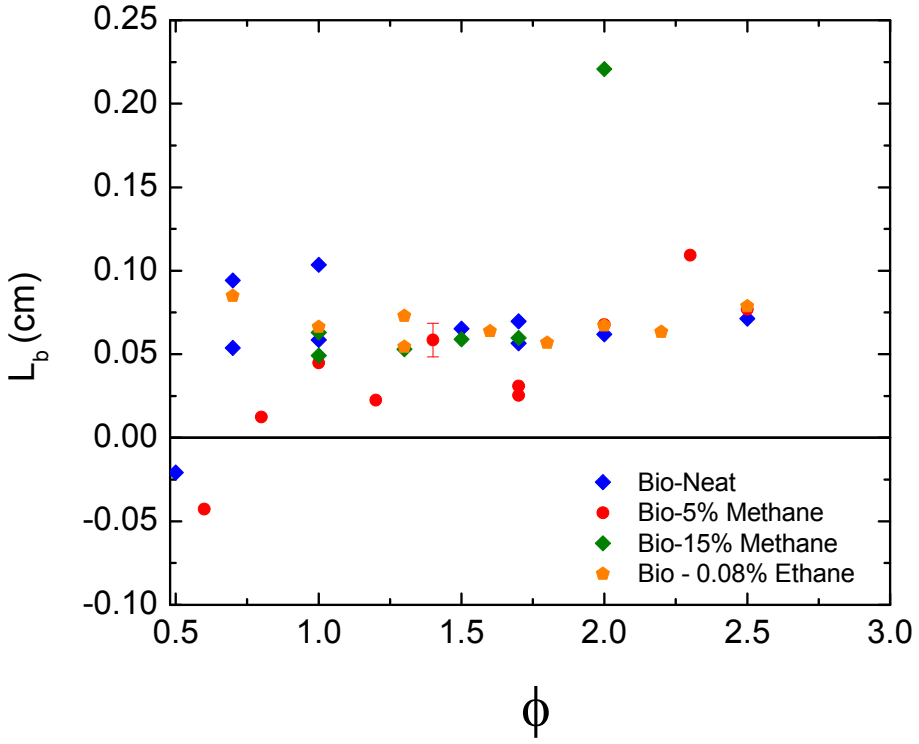

Figure 22. Burned-gas Markstein lengths for bio-syngas blends with and without hydrocarbon addition to the baseline mixture at 1 atm and initial temperature of 296 K.

The Markstein lengths calculated in this study for the neat mixture are close to those reported by Prathap et al. for syngas blends [27]. When looking at reported Markstein lengths it is important to look at the general trend of the data. Chen et al. [17] found that reported Markstein lengths could vary by more than 300% from group to group. With this large potential for variation in mind the estimated uncertainty, based on regression statistics, as seen in Lowry et al. [23], in the calculated Markstein length is ± 0.01 cm.

6.7 Lewis Number

Calculating the Lewis number of a fuel mixture can vary from study to study in the literature depending on the definition used. Bouvet et al. [28] used the definition of the ratio of thermal diffusivity to mass diffusivity of the deficient species. This definition means that it will switch from the fuel to the oxidizer as the mixture transforms from lean to rich. They also found that there were several proposed, effective Lewis number-formulations that could be used in fuel mixtures. In the present study, Lewis numbers were calculated using the chemical equilibrium function in COSILAB, and the volumetric-based effective Lewis number calculation from [28].

$$Le_V = \sum X_i Le_i \tag{6.5}$$

As seen in equation 5.1 the derived volumetric Lewis number uses the mole fractions of the deficient species multiplied by the individual Lewis number, all summed up to achieve the volumetric Lewis number.

One of the benefits of the chemical equilibrium solver in COSILAB is that it provides Lewis numbers. However, the given Lewis numbers themselves are not straight forward. They are for one mole of given species diffused into the mixture in equilibrium. This requires that when running the equilibrium calculation neglecting whatever species you are interested in, i.e. for lean mixtures excluding the fuel. This process is very simple when calculating for lean mixtures as all experiments are based on a single kmole of fuel basis, and the mole fractions are known. For rich mixtures, with oxygen as the

deficient species, the input quantities were adjusted to allow for 1 kmole of oxygen to be diffused into the mixture.

As was seen with the Lewis Number of pure hydrogen in air in the study by Hu et al. [29], the Lewis Number jumps from below unity to above unity as the mixture crosses φ = 1. This step increase is due to the deficient species changing from the fuel in the mixture to the oxygen as the mixture stoichiometry changes from fuel lean to fuel rich.

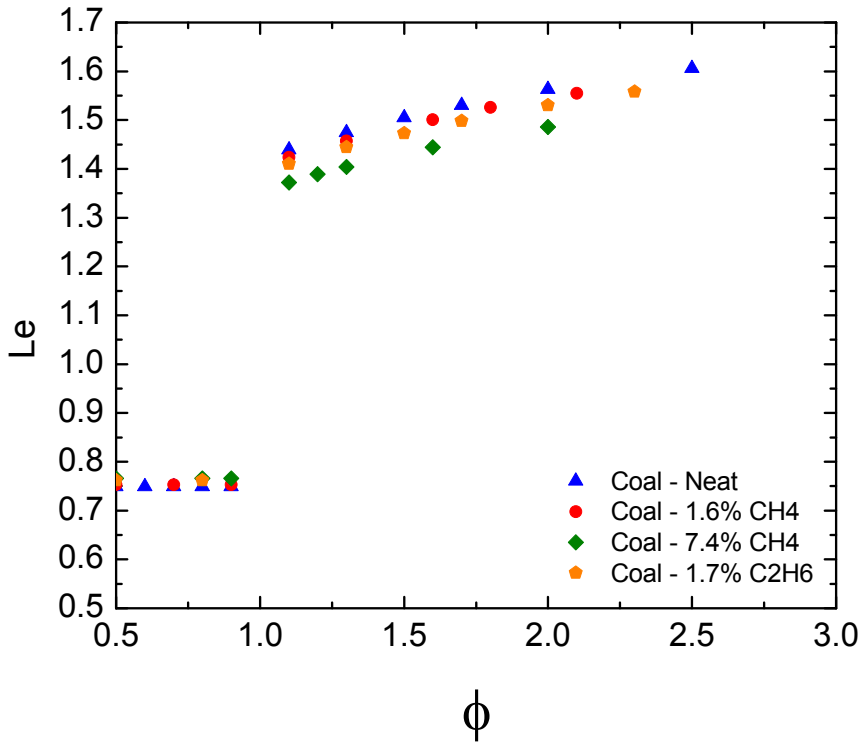

Figure 23. Lewis numbers for coal syngas blends with and without hydrocarbon addition at various equivalence ratios at 1 atm and 296 K.

The Lewis numbers for the coal-derived blends are shown in Figure 23. There is very little deviation amongst the Lewis numbers of the lean mixtures. All the blends were found to have a relatively constant Lewis number throughout the lean equivalence ratios investigated, near 0.75. As hydrocarbons were added, the Lewis number slightly increased, moving it toward unity. The same trend can be seen in the bio-syngas blends, shown in Figure 24. However as there is more hydrogen in the mixtures, and over twice as much CH_4 in the rich case, the Lewis numbers deviate slightly more for those mixtures. The Lewis number values less than unity on the lean side tend to support the trends mentioned above wherein the leaner flames tended to be less stable.

The Lewis numbers for the fuel rich equivalence ratios show a similar trend. Like the fuel lean cases, it was found that the addition of hydrocarbons moved the Lewis number closer to unity. Similar to the flame speed, the effects of the hydrocarbon addition are much more pronounced at the fuel rich equivalence ratios. The Lewis number was also found to increase for all mixtures as the equivalence ratio increased, ranging from values near 1.4 to 1.6 ($\varphi = 2.5$).

The Lewis Number of all syngas mixtures in this study is closer to 1.0 than are the Lewis numbers for pure Hydrogen reported in Hu et al. [29]. For their lean mixtures, they found the Lewis number to be around 0.3, and for the rich mixtures around 2.0. Therefore, the most-significant impact on the Lewis number is the addition of the carbon monoxide, which also has a significantly greater concentration in the fuel blends than any of the hydrocarbons added to the neat syngas mixtures.

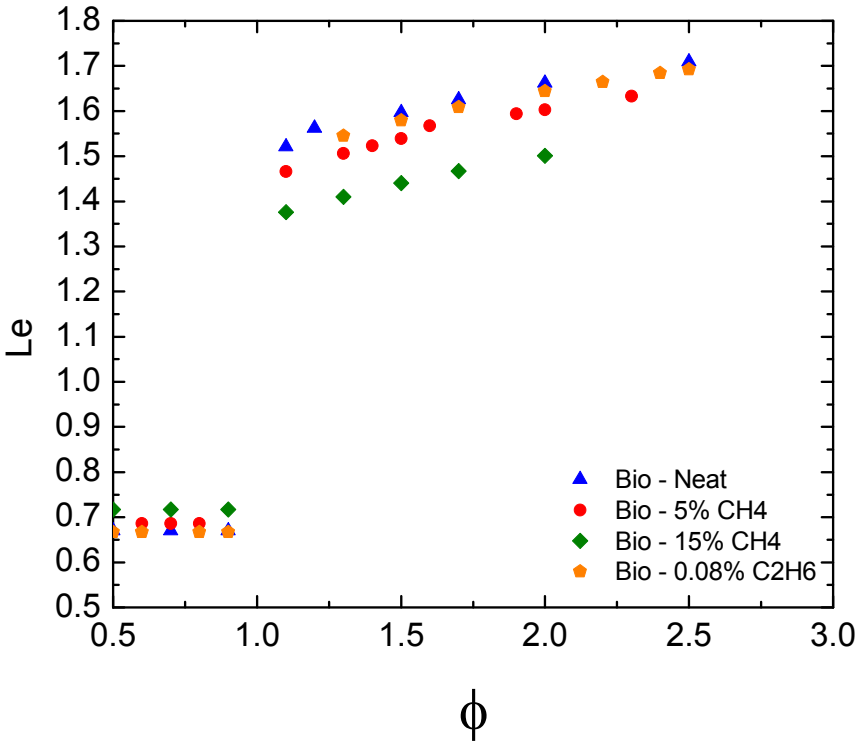

Figure 24. Lewis numbers for bio-syngas blends with and without hydrocarbon addition at various equivalence ratios at 1 atm and 296 K.

7. CONCLUSIONS

Hydrocarbon addition significantly impacts the flame speed of syngas blends. This decelerating effect is especially noticeable for rich mixtures. The model does a very good job of predicting the flame speed for the syngas mixtures in the neat case. When hydrocarbons are added, the model still does a good job of predicting the general shape of the curve and accurately predicts the equivalence ratio of the peak flame speed. However, experiments presented herein led to the finding that when hydrocarbons were added, the model under predicts the flame speed by several percent. This under prediction is especially noticeable at the richer mixtures. While the current AramcoMech kinetics model under predicts the flame speed for syngas with hydrocarbon addition, it still does a very good job for the pure fuels involved.

Analysis of the flame images found that lean mixtures were typically less stable than the fuel rich ones. The addition of hydrocarbons was found to noticeably increase the flame stability. Hydrocarbon addition however was found to have little impact on the burned-gas Markstein lengths of the mixtures. The leanest mixtures tested were the only ones to show a negative Markstein length. On average, all mixtures had a consistent Markstein length with the bio-syngas mixtures having a noticeably wider deviation. The Lewis numbers of the mixtures were found to also be consistent. For the leaner cases, there was almost no change as hydrocarbons were added, although there was a slight change toward unity Lewis Number. For the rich mixtures, the Lewis number moved noticeably closer to 1.0 as hydrocarbons were added. In general, hydrocarbon addition

seems to increase the stability of the flame. This result of hydrocarbon addition to the syngas mixture is especially important in the fuel lean regions which will typically be used in gas turbine and other industrial applications.

As stated at the beginning this work only investigated the individual effects of hydrocarbon addition. It is known that some or all of these effects could be present in real syngas mixtures. Future work will look at the effects of these added together. Also the effects of other impurities, such as the sulfur-based species, still need to be investigated.

REFERENCES

[1] Mathieu, O., Hargis, J.W., Petersen, E.L. Bugler, J., Curran, H.J., and Güthe, F., 2014, "The Effect of Impurities on Ignition Delay Times and Laminar Flame Speeds of Syngas Mixtures at Gas Turbine Conditions," ASME Turbo Expo, Düsseldorf, Germany.

[2] Lee, H. C., Jiang, L. Y., and Mohamad, A. A., 2014, "A Review on the Laminar Flame Speed and Ignition Delay Time of Syngas Mixtures," International Journal of Hydrogen Energy, 39(2), pp. 1105-1121.

[3] Mathieu, O., Petersen, E.L., Heufer, A., Donohoe, N., Metcalfe, W., Curran, H.J., Güthe, F., and Bourque, G.,, 2014, "Numerical Study on the Effect of Real Syngas Compositions on Ignition Delay Times and Laminar Flame Speeds at Gas Turbine Conditions," Journal of Engineering for Gas Turbines and Power, 136, pp. 011502-1-011502-9.

[4] Lowry, W. B., 2010, "Effect of Blending on High Pressure Laminar Flame Speed Measurments, Markstein Lengths, and Flame Stability of Hydrocarbons," Master of Science Thesis, Texas A&M University.

[5] Wender, I., 1996, "Reactions of Synthesis Gas," Fuel Processing Technology, 48(3), pp. 189-297.

[6] Hassan, M. I., Aung, K. T., and Faeth, G. M., 1997, "Properties of Laminar Premixed CO/H_2/Air Flames at Various Pressures," Journal of Propulsion and Power, 13(2), pp. 239-245.

[7] Goswami, M., Bastiaans, R. J. M., Konnov, A. A., and de Goey, L. P. H., 2014, "Laminar Burning Velocity of Lean H_2–CO Mixtures at Elevated Pressure Using the Heat Flux Method," International Journal of Hydrogen Energy, 39(3), pp. 1485-1498.

[8] Bouvet, N., Chauveau, C., Gökalp, I., and Halter, F., 2011, "Experimental Studies of the Fundamental Flame Speeds of Syngas (H_2/CO)/Air Mixtures," Proceedings of the Combustion Institute, 33(1), pp. 913-920.

[9] Das, A. K., Kumar, K., and Sung, C.-J., 2011, "Laminar Flame Speeds of Moist Syngas Mixtures," Combustion and Flame, 158(2), pp. 345-353.

[10] Burbano, H. J., Pareja, J., and Amell, A. A., 2011, "Laminar Burning Velocities and Flame Stability Analysis of H_2/CO/Air Mixtures with Dilution of N_2 and CO_2," International Journal of Hydrogen Energy, 36(4), pp. 3232-3242.

[11] Gersen, S., Darmeveil, H., and Levinsky, H., 2012, "The Effects of CO Addition on the Autoignition of H_2, CH_4 and CH_4/H2 Fuels at High Pressure in an RCM," Combustion and Flame, 159(12), pp. 3472-3475.

[12] Monteiro, E., Bellenoue, M., Sotton, J., Moreira, N. A., and Malheiro, S., 2010, "Laminar Burning Velocities and Markstein numbers of Syngas–Air Mixtures," Fuel, 89(8), pp. 1985-1991.

[13] Natarajan, J., Lieuwen, T., and Seitzman, J., 2007, "Laminar Flame Speeds of H_2/CO Mixtures: Effect of CO_2 Dilution, Preheat Temperature, and Pressure," Combustion and Flame, 151(1–2), pp. 104-119.

[14] Xu, D., Tree, D. R., and Lewis, R. S., 2011, "The Effects of Syngas Impurities on Syngas Fermentation to Liquid Fuels," Biomass and Bioenergy, 35(7), pp. 2690-2696.

[15] Krejci, M. C., Mathieu, O., Vissotski, A.J., Ravi, S., Sikes, T.G., Petersen, E.L., Kérmonès, A., Metcalfe, W., Curran, H.J,, 2013, "Laminar Flame Speed and Ignition Delay Time Data for the Kinetic Modeling of Hydrogen and Syngas Fuel Blends," Journal of Engineering for Gas Turbines and Power, 135(2), pp. 021530-021531-021503-021539.

[16] Krejci, M. C., 2012, "Devellopment of a New Flame Speed Vessel to Measure the Effect of Steam Dilution on Laminar Flame Speeds of Syngas Fuel Blends at Elevated Pressures and Temperatures," Master of Science Thesis, Texas A&M University.

[17] Chen, Z., 2011, "On the Extraction of Laminar Flame Speed and Markstein Length from Outwardly Propagating Spherical Flames," Combustion and Flame, 158(2), pp. 291-300.

[18] Metcalfe, W. K., Burke, S. M., Ahmed, S. S., and Curran, H. J., 2013, "A Hierarchical and Comparative Kinetic Modeling Study of C1 − C2 Hydrocarbon and Oxygenated Fuels," International Journal of Chemical Kinetics, 45(10), pp. 638-675.

[19] Ravi, S., Sikes, T. G., Morones, A., Keesee, C. L., and Petersen, E. L., 2015, "Comparative Study on the Laminar Flame Speed Enhancement of Methane with Ethane and Ethylene Addition," Proceedings of the Combustion Institute, 35(1), pp. 679-686.

[20] Moffat, R. J., 1988, "Describing the Uncertainties in Experimental Results," Experimental Thermal and Fluid Science, 1(1), pp. 3-17.

[21] Mueller, C. J., 2005, "The Quantification of Mixture Stoichiometry When Fuel Molecules Contain Oxidizer Elements or Oxidizer Molecules Contain Fuel Elements," SAE Trans., 114, pp. SAE Paper 2005-2001-3705.

[22] Law, C. K., Wu, F., Egolfopoulos, F. N., Gururajan, V., and Wang, H., 2014, "On the Rational Interpretation of Data on Laminar Flame Speeds and Ignition Delay Times," Combustion Science and Technology, 187(1-2), pp. 27-36.

[23] Lowry, W. B., Serinyel, Z., Krejci, M. C., Curran, H. J., Bourque, G., and Petersen, E. L., 2011, "Effect of Methane-Dimethyl Ether Fuel Blends on Flame Stability, Laminar Flame Speed, and Markstein Length," Proceedings of the Combustion Institute, 33(1), pp. 929-937.

[24] Keesee, C. L., Petersen, E.L., Zhang, K. Curran, H.J., 2015, "Laminar Flame Speed Measurments of Synthetic Gas Blends with Hydrocarbon Impurities," ASME Turbo Expo, Montreal, Canada.

[25] Santner, J., Haas, F. M., Ju, Y., and Dryer, F. L., 2014, "Uncertainties in Interpretation of High Pressure Spherical Flame Propagation Rates Due to Thermal Radiation," Combustion and Flame, 161(1), pp. 147-153.

[26] Burke, M. P., Chen, Z., Ju, Y., and Dryer, F. L., 2009, "Effect of Cylindrical Confinement on the Determination of Laminar Flame Speeds Using Outwardly Propagating Flames," Combustion and Flame, 156(4), pp. 771-779.

[27] Prathap, C., Ray, A., and Ravi, M. R., 2008, "Investigation of Nitrogen Dilution Effects on the Laminar Burning Velocity and Flame Stability of Syngas Fuel at Atmospheric Condition," Combustion and Flame, 155(1–2), pp. 145-160.

[28] Bouvet, N., Halter, F., Chauveau, C., and Yoon, Y., 2013, "On the Effective Lewis Number Formulations for Lean Hydrogen/Hydrocarbon/Air Mixtures," International Journal of Hydrogen Energy, 38(14), pp. 5949-5960.

[29] Hu, E., Huang, Z., He, J., and Miao, H., 2009, "Experimental and Numerical Study on Laminar Burning Velocities and Flame Instabilities of Hydrogen–Air Mixtures at Elevated Pressures and Temperatures," International Journal of Hydrogen Energy, 34(20), pp. 8741-8755.

APPENDIX

Table A 1. Complete Experimental Results for Syngas Blends Investigated.

Bio Syngas Baseline

FM Run	ϕ	S_L	L_b	Temp	U_{SL}
		cm/s	cm	K	
545	0.5	31.4	-0.0209	----	5.8
556	0.7	68.2	0.0538	296.0	5.8
562	0.7	70.7	0.0943	297.7	5.9
541	1	117.4	0.1035	295.3	6.0
542	1	113.7	0.0586	294.8	6.0
543	1.5	168.5	0.0654	295.2	6.1
547	1.7	180.0	0.0565	296.7	6.1
564	1.7	182.3	0.0698	297.4	6.1
544	2	187.9	0.0620	295.2	6.1
546	2.5	184.5	0.0713	296.4	6.2

Coal Syngas Baseline

FM Run	ϕ	S_L	L_b	Temp	U_{SL}
		cm/s	cm	K	
555	0.5	23.8	-0.1692	296.3	5.8
551	0.7	54.1	-0.0257	297.3	5.8
548	1	96.4	0.0501	297.2	5.9
558	1	95.2	0.0434	296.5	5.9
554	1.2	117.3	0.0514	296.0	6.0
549	1.5	142.9	0.0459	297.2	6.0
561	1.5	142.7	0.0516	297.9	6.0
553	1.7	155.3	0.0514	295.8	6.0
550	2	162.7	0.0504	297.4	6.1
563	2	166.5	0.0675	297.2	6.1
557	2.2	167.1	0.0658	296.2	6.1
552	2.5	162.0	0.0417	296.3	6.1

Bio 15% CH4

FM Run	ϕ	S_L	L_b	Temp	U_{SL}
		cm/s	cm	K	
572	1.0	89.2	0.063	293.9	5.8
582	1.0	87.4	0.0493	293.8	5.8
577	1.3	108.5	0.0408	294.0	5.9
581	1.3	110.1	0.053	294.6	5.9
573	1.5	107.5	0.059	294.2	5.9
578	1.7	89.0	0.0597	294.3	5.9
579	2.0	41.9	0.2208	294.1	5.9

Coal 7.4% CH4

FM Run	ϕ	S_L	L_b	Temp	U_{SL}
		cm/s	cm	K	
565	1.0	85.9	0.0381	294.0	5.9
568	1.3	114.1	0.0352	293.9	5.9
566	1.5	133.7	0.105	293.8	5.9
580	1.5	128.0	0.0644	294.5	5.9
570	1.7	125.8	0.0423	294.2	5.9
569	2.0	111.4	0.0628	294.1	6.1
571	2.5	48.1	0.2222	293.9	6.3

Bio 5% CH4

FM Run	ϕ	S_L	L_b	Temp	U_{SL}
		cm/s	cm	K	
600	0.6	40.6	-0.0472	296.2	5.8
595	0.8	74.11	0.0124	296.4	5.9
593	1.0	103.4	0.0449	296.6	5.9
596	1.2	125.3	0.0226	296.7	6.0
594	1.4	146.5	0.0585	296.6	6.0
598	1.7	153.1	0.031	296.6	6.0
602	1.7	153.9	0.0253	296.2	6.0
597	2.0	146.5	0.0677	296.9	6.2
599	2.3	121.3	0.1094	296.9	6.5
601	2.5	87.59	0.0769	296.3	6.7

Coal 1.6% CH4

FM Run	ϕ	S_L	L_b	Temp	U_{SL}
		cm/s	cm	K	
583	0.5	22.8	-0.0732	296.2	5.8
589	0.6	38.6	-0.0297	296.6	5.8
587	0.8	67.9	0.0238	296.8	5.8
584	1.0	95.5	0.065	296.4	5.9
591	1.3	125.5	0.0549	296.9	6.0
585	1.5	139.7	0.0504	296.3	6.0
590	1.7	151.1	0.0582	296.7	6.0
586	2.0	154.1	0.0381	296.5	6.0
592	2.0	156.5	0.049	296.6	6.0
588	2.5	144.0	0.0379	296.6	6.2

Bio Ethane (0.8%)

FM Run	ϕ	S_L	L_b	Temp	U_{SL}
		cm/s	cm	K	
605	0.7	67.7	0.0849	297.0	5.8
603	1.0	110.8	0.0663	296.5	6.0
604	1.3	144.4	0.0544	296.8	6.0
611	1.3	147.8	0.073	296.6	6.0
606	1.6	168.6	0.0637	296.5	6.0
609	1.8	175.0	0.0568	296.6	6.0
607	2.0	176.4	0.0672	296.7	6.1
610	2.2	172.3	0.0633	296.5	6.1
608	2.5	161.2	0.0786	296.5	6.3

Coal Ethane (1.7%)

FM Run	ϕ	S_L	L_b	Temp	U_{SL}
		cm/s	cm	K	
620	0.7	56.0	0.0872	297.0	5.8
617	0.9	79.869	0.0458	296.6	5.9
612	1.1	101.5	0.0495	296.6	5.9
613	1.4	129.5	0.062	296.8	5.9
619	1.4	128.5	0.057	296.7	5.9
614	1.7	142.8	0.0548	296.5	5.9
616	2.0	142.3	0.0391	296.6	6.0
615	2.3	134.0	0.0647	296.4	6.1
618	2.5	120.1	0.0620	297.2	6.3